

TagFi: Locating Ultra-Low Power WiFi Tags Using Unmodified WiFi Infrastructure

ELAHE SOLTANAGHAEI, Carnegie Mellon University

ADWAIT DONGARE, Carnegie Mellon University

AKARSH PRABHAKARA, Carnegie Mellon University

SWARUN KUMAR, Carnegie Mellon University

ANTHONY ROWE, Carnegie Mellon University

KAMIN WHITEHOUSE, University of Virginia

Tag localization is crucial for many context-aware and automation applications in smart homes, retail stores, or warehouses. While custom localization technologies (e.g RFID) have the potential to support low-cost battery-free tag tracking, the cost and complexity of commissioning a space with beacons or readers has stifled adoption. In this paper, we explore how WiFi backscatter localization can be realized using the existing WiFi infrastructure already deployed for data applications. We present a new approach that leverages existing WiFi infrastructure to enable extremely low-power and accurate tag localization relative to a single scanning device. First, we adopt an ultra-low power tag design in which the tag blindly modulates ongoing WiFi packets using On-Off Keying (OOK). Then, we utilize the underlying physical properties of multipath propagation to detect the passive wireless reflection from the tag in the presence of rich multipath propagations. Finally, we localize the tag from a single receiver by forming a triangle between the tag reflection and the LoS path between the two WiFi transceivers. We implement TagFi using a customized backscatter tag and off-the-shelf WiFi chipsets. Our empirical results in a cluttered office building demonstrate that TagFi achieves a median localization accuracy of 0.2m up to 8 meters range.

CCS Concepts: • **Networks** → **Location based services**.

Additional Key Words and Phrases: Object localization, CSI, Channel State Information, WiFi, multipath propagation

ACM Reference Format:

Elahe Soltanaghaei, Adwait Dongare, Akarsh Prabhakara, Swarun Kumar, Anthony Rowe, and Kamin Whitehouse. 2021. TagFi: Locating Ultra-Low Power WiFi Tags Using Unmodified WiFi Infrastructure. *Proc. ACM Interact. Mob. Wearable Ubiquitous Technol.* 5, 1, Article 34 (March 2021), 29 pages. <https://doi.org/10.1145/3448082>

1 INTRODUCTION

This paper asks "*Can we accurately locate ultra-low-power tags using existing WiFi infrastructure?*". Given the amount of ambient WiFi traffic in most environments, a localization system can benefit from using commodity WiFi devices to locate the backscatter signal from an ultra-low-power WiFi tag. Unlike RFID-based localization systems that require large deployments and expensive instrumentation, a WiFi backscatter system can leverage pre-existing WiFi infrastructure and devices. For example, consider the scenarios illustrated in Figure 1, where a person desires to easily locate his/her personal items such as keys, wallets, tools, or even toys in any arbitrary

Authors' addresses: Elahe Soltanaghaei, Carnegie Mellon University, esoltana@andrew.cmu.edu; Adwait Dongare, Carnegie Mellon University, adongare@andrew.cmu.edu; Akarsh Prabhakara, Carnegie Mellon University, aprabhak@andrew.cmu.edu; Swarun Kumar, Carnegie Mellon University, swarun@cmu.edu; Anthony Rowe, Carnegie Mellon University, agr@ece.cmu.edu; Kamin Whitehouse, University of Virginia, Whitehouse@virginia.edu.



This work is licensed under a Creative Commons Attribution International 4.0 License.

© 2021 Copyright held by the owner/author(s).

2474-9567/2021/3-ART34

<https://doi.org/10.1145/3448082>

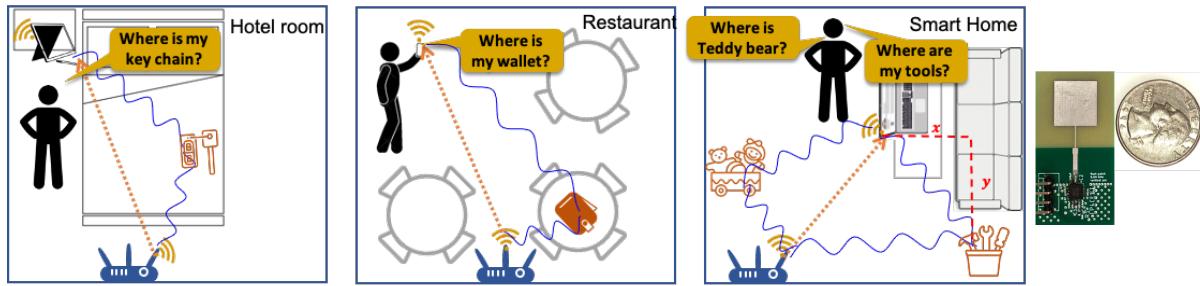


Fig. 1. TagFi's deployability and Single-point localization capabilities provides users with a WiFi-based object finding in any arbitrary environment without requiring a localization infrastructure in place.

environment such as home, hotel, or in restaurant. By having an ultra-low power WiFi tag attached to these objects of interest, one can find them by only using their personal WiFi-enabled devices such as a laptop or phone paired with the available WiFi access points without requiring any localization infrastructure in place.

In spite of the promising outcomes, achieving this vision is especially challenging due to a combination of two practical factors. First, the users have limited control and instrumentation capabilities inside a new environment. Second, they have a few personal handhelds (e.g. laptop, phone, tablets) to run the localization algorithms, so ideally we need a single-point localization approach that can locally estimate the object location by just leveraging a pre-existing WiFi access point. This naturally rules out RFID-based systems as they require dense deployment of expensive and specialized readers, which may not exist in any arbitrary environment such as hotels or restaurants. While Bluetooth-based solutions such as Tile tags [1] or UWB tags [2] are infrastructure-free and can operate in recent smart phones, the tags are too power hungry with maximum of one year life-time and only provide proximity information and not 2D location. A WiFi-based object localization can potentially satisfy all these requirements, however, existing WiFi backscattering solutions either: (1) use specialized hardware [8, 21, 22] that imitate the RFID reader in full-duplex operation; or, (2) use techniques such as frequency shifting or coordinated localization between multiple devices, which are not compatible with natural operation of WiFi protocols and devices [24, 46, 56].

More specifically, the main challenge in WiFi backscattering is that the backscatter signal from the tag is considerably weaker than the Line-of-Sight (LoS) path between two WiFi devices, which can push the tag reflection below the noise floor. This becomes even more challenging in rich multipath environments with signals reflecting off of walls and furniture with people moving around. As such, the tag reflection does not create distinctive difference in the channel measurements. The solution used in the literature to address this challenge is to design the tag such that it shifts the frequency of the backscatter signal to a side band, thus isolating the tag reflection from dominant multipath signals. However, this requires the WiFi transmitter and receiver to operate in different frequency channels, or the installation of an extra WiFi chipset at the receiver to listen to the new frequency band of tag operation, both leading to an impractical situation in existing WiFi infrastructure. In addition, the required high frequency oscillator for frequency shifting increases the tag's power consumption.

In contrast to these past systems that unnaturally require the receiver to switch to a different frequency, we present *TagFi*, a new backscatter localization system, that allows the WiFi transmitter, receiver, and the tag to all operate on one common frequency, as is typical in WiFi. As a result, it can work with existing WiFi infrastructure, making deployment much more practical. The natural consequence of the tag operating on the same frequency of operation would be reduced tag range, due to high in-band interference. However, we investigate if at least some

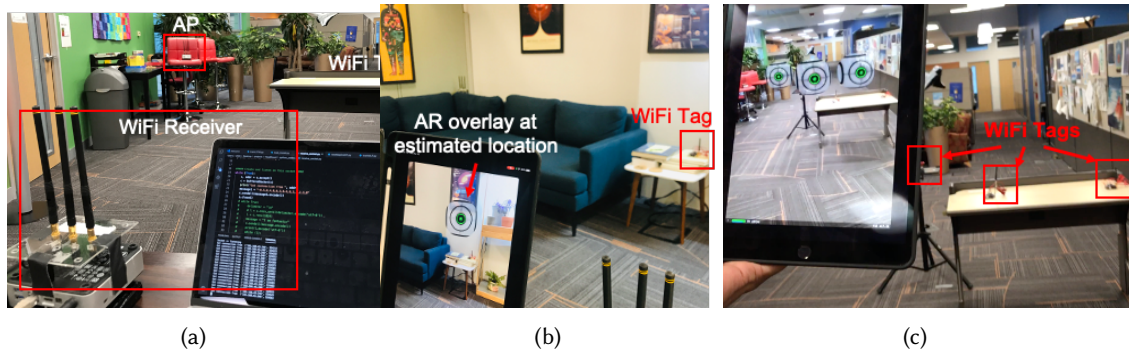


Fig. 2. TagFi in action. Snapshots of TagFi’s (a) experimental setup, (b) AR interface at the mobile device, (c) multi-tag localization output

of these losses can be improved through more powerful signal processing techniques at the receiver, trading off a modest reduction in tag range for a much more practical and deployment-ready system.

TagFi’s tag design uses the least restrictive backscatter protocol that blindly modulates any ambient WiFi signal, and focus on detecting and locating these concurrent signals at the receiver. TagFi uses Channel State information (CSI), which is collected by commercial WiFi chipsets. Since CSI is measured from the packet preamble, it can localize a tag by just eavesdropping ongoing WiFi traffic, and so, piggyback localization on regular WiFi communication with minimum to zero impact on wireless networks. In addition, a single WiFi device (e.g. laptop, desktop computer, etc) can localize the tag by forming a multipath triangle between the tag and any arbitrary WiFi transmitter, e.g. the WiFi Access Point (AP), sending the ambient traffic without requiring triangulation with multiple nodes. Consider the potential benefits of such single-point WiFi-compatible design. One could envision an ultra low-power tag free of any computational logic attached to objects for tracking and localizing it in any new environment even if only one pre-existing WiFi access point is within range.

In spite of the simplicity and elegance of this solution, it comes with major challenges. First, the lack of a MAC protocol as well as the asynchrony of the tag and WiFi transceivers requires the tag to continuously backscatter any existing WiFi signals. This could potentially increase the tag’s power consumption and drain battery. To address this challenge, TagFi minimizes the power consumption of the tag by using a simple RF switch that toggles the internal impedance to either reflect or absorb the incident signal. Such a design needs no envelop detector, decoding, packet buffers or high-speed RF oscillator, which leads to a power consumption of 16uW, translating to 3.6 years of operating on a 3V lithium coin cell by using the switching frequency of 200Hz.

The second challenge is that without frequency shifting, the backscatter path and other multipath signals occupy the same channel, resulting in high dynamic range and high in-band interference. To address this challenge, TagFi leverages the spatial structure of the modulated backscatter signal to pull the signal above the noise floor. The high level intuition is that the tag modulated reflection is incoherent with the rest of multipath signals, which stands out in subspace super-resolution method [37]. Therefore, to separate the tag reflection from other multipath signals, we adapt a MUSIC-based super resolution algorithm (described in Section 3.2) to explicitly look for a path that is modulated. We show that this code-optimized MUSIC algorithm can detect the backscatter signals that are significantly weaker than the LoS path, even in dynamic environments with the presence of mobile paths. Finally, TagFi triangulates the position of the tag by measuring the angle of arrival (AoA) and angle of departure (AoD) of the tag reflection, and derives the tag’s modulation code as tag ID.

We create multiple prototypes of the WiFi tag, one using off-the-shelf components and the others with customized hardware and on-board PCB antenna optimized for ultra low-power operations. We also implement

TagFi using Intel 5300 WiFi chips as our WiFi transmitter and receiver, operating at 5GHz with 40MHz bandwidth and equipped with a 3-element linear antenna array. We deploy TagFi in an office building and evaluate its performance in multiple scenarios, in the presence of multiple tags, and different mobility scenarios. Our empirical results show that TagFi achieves a median localization accuracy of 0.2m up to 8 meters range. This is comparable with the best existing WiFi localization systems, all of which require an active WiFi radio on the object and coordination between multiple APs.

Applications. TagFi’s key advantage is the ability to operate in any new environment getting a power-boost from any pre-existing WiFi access point paired with a personal device of the user such as a laptop or tablet. As a result, TagFi can deliver the many well-studied localization applications of RFID tags without the deployment hassle. A few such applications include: (1) *Object Finding*: Finding objects of interest (toys, tools, medicine, keys, etc.) in a new environment one steps into such as a hotel room; (2) *Augmented Reality*: Using TagFi tags for calibration and context awareness from an Augmented Reality helmet that is already WiFi enabled, even if in low visibility conditions or when the tags are not in direct-field of view – unlike for example, April Tags. (3) *Tracking Wearables*: Using TagFi tags attached to the body for gesture sensing, fitness tracking, fall detection, etc. in any environment where WiFi is available.

Scope and Limitations. (1) TagFi assumes that both the WiFi access point and receiver have multiple antennas (i.e. are MIMO-capable). We note that most laptops, tablets and increasingly smartphones are MIMO capable. (2) TagFi performs location tracking in 2D space. Performing 3D localization from a single transmitting and receiving WiFi pair, each with linearly spaced antennas is a known to be theoretically impossible [42], owing to the absence of sufficient degrees-of-freedom to resolve the third dimension. While this can potentially be resolved by aggregating information across multiple vantage points (e.g. multiple WiFi clients), it is beyond the scope of this paper. (3) TagFi shares some limitations common to RF backscatter systems – it operates at ranges of 6-8 meters and is vulnerable to persistent and complete blockages that further weaken the signal. We do however, evaluate the system under temporary blockages and environmental dynamics.

Contributions: The main contributions of this paper include:

- *TagFi*: a novel tag localization and identification system that only uses the existing WiFi infrastructure and commodity wireless devices. So, it fully piggybacks tag localization on regular WiFi communications without requiring devices to operate in different frequency channels.
- *Asynchronous tag design*: We use a tag design that is fully asynchronous in favor of practicality, which enables a minimal architecture at the tag while addressing the high in-band interference with more powerful signal processing techniques at the receiver.
- *Code-optimized super resolution*: TagFi leverages the backscatter modulation and spatial structure of the signal to overcome complex multipath interference. This enables extracting a weak wireless reflection in the presence of strong line-of-sight path. While this method is general, we show that it enables tag localization with no need for complex operations at the tag such as frequency shifting.
- *Single-point localization*: TagFi provides decimeter-level tag localization from a single channel in a single WiFi receiver. So, combined with asynchronous tag architecture and its compatibility with existing WiFi infrastructure, it enables a new primitive of ubiquitous and infrastructure-less sensing and localization.

2 BACKGROUND AND RELATED WORK

TagFi is related to previous works in three areas: localization of commercial RFID tags, device localization of WiFi radios, and backscatter communication. In what follows, we discuss how TagFi fits into related works.

Table 1. Compared to the state-of-the-art of localization systems, TagFi is the only solution that provides single-point localization and is fully compatible with existing WiFi infrastructure with no need for high power operations at the tag such as frequency shifting.

	Ultra-low Power Tag	Single Point Localization	Compatible with Existing Infrastructure	Work on Commodity WiFi Devices
WiTag [24]	✗	✗	✗	✓
OFDMA [44]	✓	✗	✗	✓
RFind [29]	✓	✗	✗	✗
MonoLoco [42]	✗	✓	✓	✓
TagFi	✓	✓	✓	✓

RFID-based Localization. With RFID technology, one can track battery-free objects by attaching a passive tag. In these systems, a tag backscatters the excitation signal transmitted by an RFID reader and encodes its own information on the reflected signal. The phase and amplitude of the backscattered signal is then used for localizing the tag by either calculating the received signal strength (RSS) [9, 10, 35, 60], the time of flight based on phase measurements [4, 28, 47, 48, 54], or the angle of arrival (AoA) using multiple antennas [6, 17, 25, 30, 61]. However, to deal with multipath interferences, these methods require either a dense deployment of reference tags in the area of interest [33], leveraging a moving reader’s antenna to create a synthetic aperture radar [48], or frequency hopping across all RFID channels [29] to emulate a wider bandwidth. Additionally, all these RFID-based approaches require dedicated infrastructure and expensive RFID readers. In contrast, TagFi leverages the available pervasive WiFi infrastructure and enables object localization in any WiFi receiver using ambient traffic. We adapt the on-off keying modulation and transform it into a technique for identifying the weak WiFi backscatter signal in the presence of complex multipath propagations.

WiFi Backscatter Communication. The concept of utilizing the passive WiFi reflection is originally proposed for connecting ultra-low-power objects to the Internet. WiFi Backscatter [21], BackFi [8], and Passive WiFi [22] are the examples of these systems that use specialized readers for decoding WiFi backscattering signals. All of these systems either require modification on the WiFi device or specialized hardware to cancel multipath interference. The recent backscatter communication systems utilizes commodity WiFi devices, but they deal with multipath interferences by either changing the phase of the signal [57, 59] or shifting the frequency of the backscatter to a non-overlapping channel [56, 58], both of which significantly increase the power consumption of the tag. In addition, frequency-shifted backscatter requires the WiFi transmitter and receiver to operate in different channels, an impractical assumption for regular WiFi networks.

WiTag [24] and OFDMA backscatter [44] are the closest backscatter localization systems to our paper, which localize low-power tags with commodity WiFi radios. However, both of these systems use the side-band modulation (frequency shifting), which limits the performance and practicality of these systems in multiple ways. First, they unnaturally require the WiFi receiver to switch to a different frequency, potentially missing useful packets on its normal frequency of operation. Second, an explicit coordination between the two WiFi transceivers is required to agree on the secondary frequency channel as well as installation of an extra eavesdropper to listen to new frequency band, so it is not compatible with existing WiFi infrastructure. Third, shifting the signal frequency requires a high-frequency oscillator which consumes more power and is not efficient for long-time operation. In contrast, TagFi adapts an asynchronous and practical architecture that enables tag localization at a single receiver by fully using existing infrastructure.

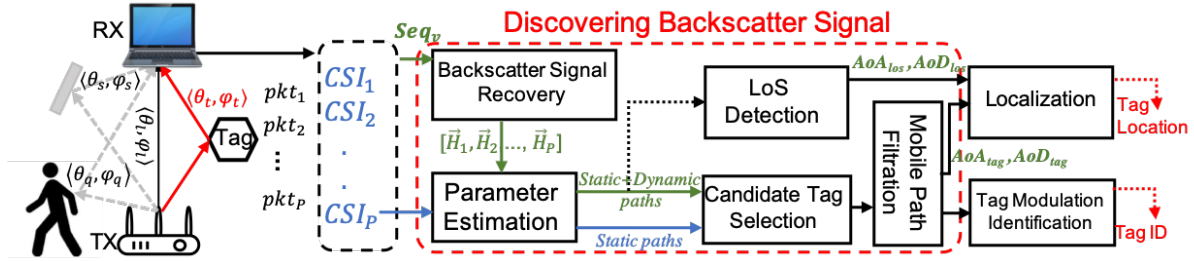


Fig. 3. System Overview of TagFi

WiFi-based Localization. Active radios such as WiFi have been extensively used for localizing devices, which require an active WiFi chipset mounted on the target. The transmitted signal is then collected by one or multiple WiFi receivers to compute the location of the target. The first generation of WiFi-based localization systems look at the received signal strength and use fingerprinting to determine the location of the target [7, 11, 12, 15, 40, 43, 50]. However, these methods require an extensive effort to characterize the environment. Recent techniques eliminate the effect of multipath interferences by directly measuring the geometric features of the line of sight (LoS) path between the target and the WiFi receiver(s). AoA-based methods [13, 18–20, 26, 36, 38, 42, 52] use an array of antennas to compute the direction of the LoS signal, while ToF-based methods [12, 14, 27, 31, 32, 41, 55] use either signal measurements from multiple frequency channels or round trip propagation time to estimate the distance between the transmitter and receiver. Since all of these systems require an active WiFi transceiver on the target, they are not suitable for object localization with minimal to zero sources of power. In contrast, TagFi utilizes the backscattered signal from a tag without requiring an active radio or any power hungry component.

3 SYSTEM DESIGN

TagFi is a WiFi-based object localization system, which uses ambient WiFi traffic at a single commodity WiFi receiver. A WiFi device such as a laptop or tablet that is equipped with multiple antennas, will eavesdrop the packets from an access point in the room. At the same time, the tag asynchronously backscatters the WiFi signals, which is also received at the WiFi receiver. TagFi measures the CSI values of the received packets from multiple antennas and extracts the tag reflection by exploiting the modulation of the backscatter signals across multiple packets. Finally, it localizes the tag in the 2D space relative to the WiFi receiver. As shown in Figure 3, TagFi works in three steps:

- **Backscattering modulated WiFi signals:** TagFi uses an asynchronous on-off keying modulation at the tag in favor of practicality and low power consumption. However, this results in high in-band interference of the weak backscatter signal with other multipaths. Section 3.1 explains how TagFi leverages the modulated structure of backscatter path to address this challenge and recover the tag reflection from the noise floor.
- **Discovering Backscatter Signal:** TagFi leverages the Channel State Information (CSI) measured across multiple antennas as well as over time to estimate the angular geometries of the tag reflection and the LoS path. Section 3.2 elaborates how TagFi identifies the tag reflection among other recovered paths including mobile paths.
- **Localizing the Tag:** TagFi then defines a triangle between the WiFi receiver, transmitter, and the tag. As explained in Section 3.4, it constrains the geometry of this triangle by obtaining the AoA and AoD information of the backscatter path as well as the LoS path, thus localizing the tag from a single receiver and without requiring to know the relative location of the WiFi transmitter and receiver up front.

3.1 Backscattering Modulated WiFi Signals

Backscatter signals are usually much weaker than the LoS path coming directly from the active WiFi transmitter due to extra travel time and tag's small radar cross section. Detecting the backscatter signal is even more challenging in rich multipath environments due to high dynamic range. A conventional solution to address this problem is to use frequency-shift tags that reflect the backscatter signal in an adjacent non-overlapping frequency channel. However, this solution requires WiFi devices in different frequency channels, which is not compatible with regular WiFi networks where devices operate in the same channel for data communication and they can listen to one channel at a time. To address this problem, we use a simple on-off keying (OOK) modulation that only requires an antenna and an RF switch. The switch modulates the backscatter signal at the packet level by toggling the internal impedance between *reflective* and *non-reflective* modes. The power of the backscattered signal is a function of the tag's reflection coefficient

$$\Gamma = \frac{Z_T + Z_A^*}{Z_A - Z_T} \quad (1)$$

where Z_A is the antenna impedance and Z_T is the impedance of the tag terminal. When the switch is in the impedance match state ($Z_T = Z_A^*$), the circuit acts as an open terminal and absorbs all the signal. However, when $Z_T = 0$, the switch is in impedance mismatch state, which acts as a short terminal and total reflection of the received power. As such, the tag modulates the WiFi channel between the tag and the receiver by reflecting or absorbing the WiFi packets at the same channel.

However, OOK modulation is not sufficient to detect the tag specially in longer ranges and rich multipath environments as it does not create enough distinctions on the channel measurements and potentially falls below the noise floor. To address this issue, we use the modulated structure of the backscatter signal and the measurements across time and space to effectively pull the tag reflection toward the signal subspace. The intuition is that a modulated signal is incoherent with static multipath signals (such as LoS path) over time. Let us define the wireless channel at time t , subcarrier f and antenna s as:

$$H(t, f, s) = \sum_{l=1}^L X_l(t, f, s) + N(t, f, s) \quad (2)$$

$$= \sum_{l=1}^L \Gamma_l(t, f, s) e^{-j2\pi f \tau_l(t, f, s)} + N(t, f, s) \quad (3)$$

where L is the total number of multipath components, X_l is the received signal, and Γ_l and τ_l are the complex attenuation and propagation delay of the l^{th} path, respectively. By classifying multipath signals into static group L_s and modulated group L_m , the received signal can be divided to:

$$H(t, f, s) = \sum_{l_s \in L_s} X_{l_s}(t, f, s) + \sum_{l_m \in L_m} X_{l_m}(t, f, s) * \text{rect}(t) + N(t, f, s) \quad (4)$$

where $\text{rect}(t)$ represents the square-wave nature of the tag modulation. Without loss of generality, let us consider two packets with different modulation states. So, the signal measurements of these two packets can be written as

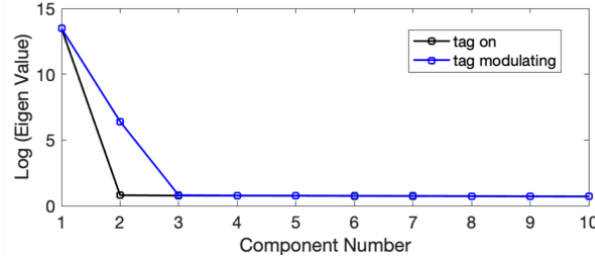


Fig. 4. Tag modulation increases the signal subspace eigenvalues which indicates the rank increase of the signal covariance matrix.

a linear combination of the same steering vectors derived from L paths, but linearly independent complex gains:

$$[H_1 H_2] = \underbrace{[e^{-j2\pi f \tau_1}, e^{-j2\pi f \tau_2}, \dots, e^{-j2\pi f \tau_{1_s+l_m}}]}_{\text{same steering vectors}} \times \underbrace{\begin{bmatrix} \Gamma_1 & \Gamma_1 \\ \cdot & \cdot \\ \cdot & \cdot \\ \Gamma_{1_s} & \Gamma_{1_s} \\ \Gamma_{1_s+1} & 0 \\ \cdot & 0 \\ \Gamma_{1_s+l_m} & 0 \end{bmatrix}}_{\text{Linearly independent gains}} \quad (5)$$

Therefore, the two packets with different modulation states will create incoherent measurements of the signal over time, so we can potentially use signal averaging over multipath packets to boost the SNR. However, a simple averaging and correlation does not work due to sampling frequency offset across WiFi packets. To address this issue, TagFi combines SNR boost and tag detection by applying a MUSIC-based technique explained in the next section.

Asynchronous Modulation. TagFi's design choice is to keep the tag as simple as possible to minimize the cost and energy consumption. Therefore, we let the tag to blindly modulate and backscatter the WiFi packets as they come, and will deal with decoding these asynchronous measurements at the WiFi receiver. The basic idea is that the tag repeatedly toggles its internal impedance using a fixed modulation rate as well as a fixed length of code, which are both known to the WiFi receiver. The receiver periodically searches for the tag by collecting packets for a time window larger than the tag's modulation period. This enables concurrent localization of a tag from different WiFi receivers. However, there is a trade off between tag's power requirements, modulation rate and the required scan time which are further discussed in Section 3.7. For the rest of this section, we first present our system by assuming a single active tag and then discuss how it can be generalized for multiple tags.

3.2 Discovering Backscatter Signal

In the previous section, we see that the tag modulation combined with signal averaging effectively decorrelates the tag signal from other multipath signals and pulls the tag reflection above the noise floor. The model presented in equation 5 creates the basis for applying sub-space methods like MUSIC [37], which are derived from signal and noise eigenvector estimates. Hence, combining signal measurements from multiple transmitting and receiving

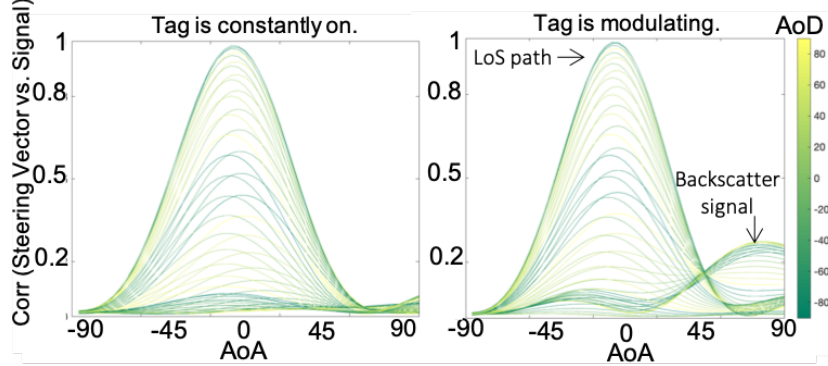


Fig. 5. Tag modulation combined with the adapted sub-space method recovers tag reflection.

antennas across multiple packets creates a new measurement matrix \mathbf{X} as:

$$\mathbf{X} = [\vec{H}_1 \vec{H}_2 \dots \vec{H}_P] \quad , \vec{H}_p = [x_{1,1}^p \dots x_{M,N}^p]^T \quad (6)$$

$$x_{m,n} = \sum_{i=1}^L \Gamma_i (e^{-j2\pi(m-1)d \sin(\theta_i)/\lambda} \times e^{-j2\pi(n-1)d' \sin(\varphi_i)/\lambda}) \quad (7)$$

where \vec{H}_p is the CSI measurements of the p^{th} packet across M receiving antennas and N transmitting antennas, d and d' are the distances between receiving and transmitting antennas, respectively. MUSIC-based algorithms perform eigenstructure analysis on the covariance matrix $R_{\mathbf{X}}$ of the P CSI samples as:

$$R_{\mathbf{X}} = \mathbb{E}[\mathbf{X}\mathbf{X}^H] = \frac{1}{P} [\vec{H}_1 \vec{H}_2 \dots \vec{H}_P] \begin{bmatrix} \vec{H}_1^* \\ \vec{H}_2^* \\ \dots \\ \vec{H}_P^* \end{bmatrix} = \frac{1}{P} \sum_{i=1}^P \vec{H}_i \vec{H}_i^* \quad (8)$$

, which in fact averages the covariance of the signal across modulated packets. Figure 4 compares the 10 largest eigenvalues of $R_{\mathbf{X}}$ for 1000 packets in two scenarios: (1) the tag is constantly on but not modulating (2) the tag is constantly modulating. The significant increase of the second eigenvalue indicates the increase of the matrix rank in the averaging process and therefore the projection of the tag reflection on signal subspace.

To separate the tag reflection from multipath signals, we adapt the super-resolution algorithms [23, 42] to estimate the geometrical parameters of multipath signals. These parameters include (1) the direction at which the signal is leaving the transmitter (known as AoD), (2) the direction at which the backscattered signal is arriving from the tag to the WiFi receiver (known as AoA), and (3) the relative Time of Flight (ToF) of the tag's reflection with respect to the LoS. It should be noted that commodity WiFi devices suffer from random phase offset due to sampling time offset (STO) and packet detection delay (PDD), which result in large ToF errors. We adapt the conventional ToF sanitization algorithms [42], which remove a linear fit of the unwrapped phase shift across subcarriers. However, this leaves only enough information to derive relative ToF between multipaths. In the next section, we demonstrate that the relative ToF is sufficient for localizing the tag. So from now on, whenever we refer to ToF, it can be substituted with *relative ToF* without loss of generality. It should be noted that these phase offsets are constant across antennas of a device due to internal time synchronization of local oscillators, so they do not affect AoA or AoD measurements.

However, there are several challenges in applying MUSIC to our context. First, except the modulated backscatter signal, the other multipath signals are highly correlated as they share the same signal source. This degrades the rank of the covariance matrix and results in spurious peaks due to random merging of coherent multipath signals. It should be noted that the conventional MUSIC algorithm uses smoothing techniques [39] to deal with high multipath correlations, however, here we intentionally skip this step and leverage the natural incoherency of the tag reflection from other multipath signals. So, to deal with spurious paths, we need to carefully filter out these false peaks and select the peaks corresponding to the LoS and tag reflection paths. To address this challenge, unlike the standard form of MUSIC that relies on the orthogonality of noise subspace and signal measurements, we alternatively exploit the signal subspace which carries the tag modulation. Given L multipath signals, the eigenvectors corresponding to the L largest eigenvalues create the signal subspace $E_S = [\vec{e}_1, \dots, \vec{e}_L]$ for which the subspace correlation will be maximized at the path geometry:

$$\text{SubCorr}(E_S, A(\theta, \varphi, \tau)) = \frac{A(\theta, \varphi, \tau)^H E_S E_S^H A(\theta, \varphi, \tau)}{A(\theta, \varphi, \tau) A(\theta, \varphi, \tau)^H} \quad (9)$$

where $\vec{A}(\theta, \varphi, \tau)$ is the path steering vector. Figure 5 shows the effectiveness of tag modulation in shifting the tag reflection toward the signal subspace, which is, consequently detectable by our adapted MUSIC algorithm. In addition, the joint estimation of AoA, AoD, and ToF allows us to create a larger sensor array. For example, measurements from 3 receiving antennas, 3 transmitting antennas and 30 subcarriers create a sensor array with 270 elements, which is significantly larger than the number of dominant paths in an indoor space. Combined with the joint-estimation signal processing techniques [45], we can further push the resolution and accuracy, from typical raw sample resolution of 7.5m for a 40Mhz bandwidth [53] to degree-level and sub-meter resolution [42, 51].

Another challenge is that strong multipath signals such as the LoS path can shadow over weaker paths specially if they are closely spaced, thus degrading the resolution of the super-resolution algorithm. This is specifically problematic in our case as the tag reflection is much weaker than the LoS path or even static reflectors in the environment. To address this issue, we apply MUSIC in an iterative manner. In each iteration, we first remove the projection of already resolved paths from both the signal subspace and steering matrix and then perform another MUSIC search to find the next path, which will be the global maxima over the modified signal subspace. Therefore, if the signal is dominated by one path (such as the LoS path), it will be removed from the signal subspace after an iteration, thus enabling the detection of weaker paths such as the tag reflection. The orthogonal projection matrix of a vector space A is calculated as

$$P_A = 1 - A(A^H A)^{-1} A^H \quad (10)$$

The number of iterations in this process is defined by L , the expected number of paths and accordingly the size of the signal spaces. We use the eigen-value thresholding heuristics proposed for sub-space algorithms to define L [45]. We note that the above algorithm is similar to [34], which localizes dipoles in the human brain from EEG and MEG measurements. TagFi uses an extension of a similar process in the AoA, AoD, and ToF dimensional space.

3.3 Dealing with Various Multipaths

After resolving the parameters of multipath signals, TagFi's next step is to identify the tag reflection among all resolved multipath signals. This is particularly challenging in the presence of both static and dynamic paths. To this end, TagFi employs the incoherent relationship of the tag's modulating reflection and static paths to distinguish it from other static paths such as reflections from walls and furniture, and uses the unique modulating pattern of the tag reflection to distinguish it from other dynamic paths. The details are explained in the following sections.

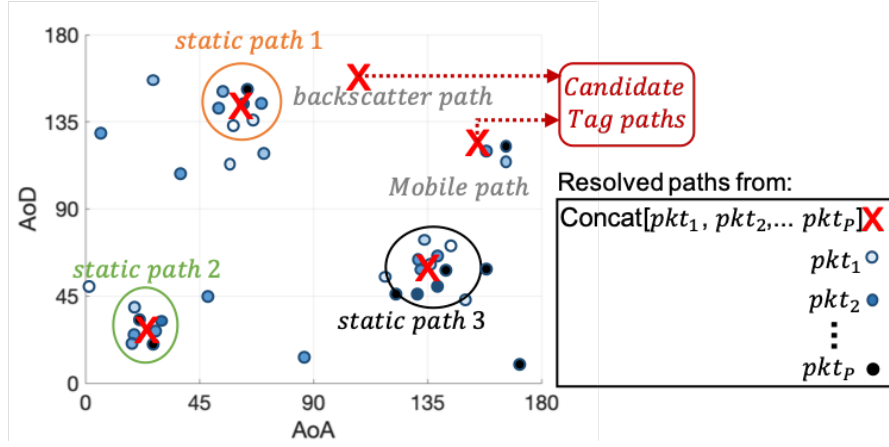


Fig. 6. TagFi extracts candidate tag paths by comparing the resolved paths from concatenated packets in a sequence vs. individual packets.

3.3.1 Selecting Candidate Tag Reflections. To identify which resolved path represents the parameters of the backscatter signal, TagFi first employs the unique feature of the tag reflection which is its modulation. As mentioned before, the backscatter signal is the only multipath component that is modulated across WiFi packets and it is only detectable if these packets are concatenated in the super-resolution algorithm. So, a candidate tag reflection is a path that is resolved from packet concatenations, but not the individual packets. The main challenge is that this process may confuse tag reflections with dynamic paths such as reflections from a mobile person or object. So, in this step, we first separate the list of candidate tag reflections and then filter out the mobile paths.

Let assume a sequence of P modulated packets. The geometric parameters of $\Phi = \{\theta_l, \varphi_l\}$ are estimated for L paths using this ensemble of the packets and the proposed adapted MUSIC. Then, TagFi finds this parameter set for each individual packet by applying the adapted MUSIC on single \vec{H}_p , which results in a set of resolved paths as

$$\bigcup_{p \in P} \bigcup_{l \in L^{(p)}} \{\theta'_l, \varphi'_l\} \quad (11)$$

As shown in Figure 6, TagFi then matches the parameters of different packets and extracts the unique elements of the above set through a clustering algorithm. This will eliminate the spurious paths resolved due to signal distortions. Then, the candidate backscatter signals are extracted by calculating the relative complement of the cluster centroids $\zeta = \{\theta'_c, \varphi'_c\}$, $\zeta \in \mathbb{C}$ derived from individual packets with respect to elements of Φ :

$$\Phi \setminus \zeta = \{ \{\theta_l, \varphi_l\} \mid l \in L \text{ and } \{\theta_l, \varphi_l\} \pm \varepsilon \notin \mathbb{C} \} \quad (12)$$

ε is the threshold used to account for the noise in measurements and the estimation variances and is set to 3° in our current implementation. It should be noted that TagFi assumes that the candidate backscatter paths are first-order reflections. In practice, there are usually more than one multipath signal incident at the tag as the emitted signal reflects off of objects before arriving at the tag. Similarly, the signal backscattered by the tag bounces off of objects and reaches the receiver along multiple paths. However, the second-order reflections are significantly attenuated and won't be among the 6-8 dominant paths resolved by the super-resolution algorithms [42].

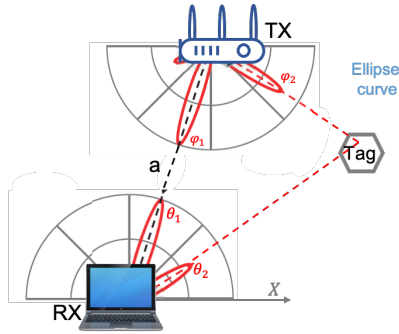


Fig. 7. Localization using AoA and AoD of the tag reflection and LoS path

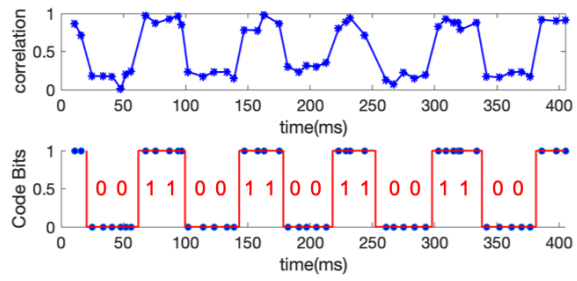


Fig. 8. TagFi uses the correlation of the steering vector and CSI of each packet to find the modulation code.

3.3.2 Mobile Path Filtration. In practice, it is necessary for a tag localization system to work robustly in a dynamic environment with people moving around. However, movement of a person introduces Doppler frequency on the reflected signal from the body, which changes the length of the path over time. This makes the mobile paths incoherent with the static paths as well as the backscatter signal, so it can be mistakenly selected as a candidate backscatter signal in the previous step. TagFi handles these cases by employing v sequences of P modulated packets and a clustering technique on their corresponding candidate tag reflections. The intuition is that the AoA and AoD of the backscatter signal have smaller variations over time compared to falsely resolved or mobile paths. TagFi first applies a K-means clustering algorithm on the collective candidate paths extracted for v sequence of P packets. Then it calculates the maximum density of each cluster using a bivariate Kernel Density Estimator (KDE) with a Gaussian kernel, which fits a 2 dimensional spatial probability density function to each cluster. The cluster with the highest density will be eventually determined as the backscatter path.

Mobility of The Tag or WiFi Devices: In mobile scenarios such as when a handheld device (e.g. tablet or laptop) is used as the WiFi reader/receiver or the user carries the tag while moving, all multipath signals experience Doppler shift, thus degrading the incoherence of the modulated backscatter signal with other paths. However, this is only problematic when the modulation frequency and the Doppler frequency fall on the same range. Given the typical walking velocity of 1m/s [3], we avoid this issue by selecting the tag modulation period between 5ms to 10ms. Therefore, the tag modulation has enough separation from potential Doppler shifts of other multipath signals.

3.4 Localizing the Target Tag

TagFi localizes the tag with the derived AoA and AoD of the backscatter path along with the ones for the LoS path between the WiFi transmitter and receiver. It defines the LoS path to be the path with the shortest ToF value since it does not go under any reflection before reaching the receiver. It is worth noting that commodity WiFi radios can only estimate the relative ToF between multipath signals due to the sampling frequency offset (SFO) and sampling time offset (STO) caused by lack of time synchronization between the two nodes. However, the relative ToF is sufficient for determining the LoS path from other reflections.

As shown in Figure 7, the LoS signal transmits with the AoD of φ_1 , propagates a distance a , and arrives at the receiver with the AoA of θ_1 . Similarly, the backscatter path from the tag has left the WiFi transmitter with the AoD of φ_2 and arrives at the WiFi receiver with AoA of θ_2 . Given these values, we denote the locations of the tag, WiFi transmitter, and receiver as (x, y) , (x_t, y_t) , and $(0, 0)$. The tag's location with respect to the receiver is then

derived from the intersection of the semi-ellipse determined by the range and the semi-line determined by AoAs:

$$x = \frac{a \sin(\varphi_1 - \varphi_2) \cos \theta_2}{\sin(\varphi_2 + \varphi_1 + \theta_1 - \theta_2)}, y = \frac{a \sin(\varphi_1 - \varphi_2) \sin \theta_2}{\sin(\varphi_2 + \varphi_1 + \theta_1 - \theta_2)} \quad (13)$$

where $a = \sqrt{x_t^2 + y_t^2}$ and is either known to the receiver or jointly estimated with the tag location using Multipath Triangulation [42]. It should be noted that Multipath Triangulation proposed in [42] jointly localizes the WiFi devices and a reflection surface. So by adapting a similar technique, we can jointly localize the WiFi transceivers as well as the tag relative to the receiver without requiring any apriori knowledge of the distance between the two WiFi devices. This is further evaluated in Section 3.4 and the end to end localization algorithm is shown in pseudo code in Algorithm 1.

In the case of having multiple WiFi transmitters in the monitoring area, we can further improve the localization performance by solving the following optimization problem:

$$\operatorname{argmin} \sum_{i=1}^Q (x_i - \hat{x})^2 + (y_i - \hat{y})^2 \quad (14)$$

where Q is the number of WiFi transmitters. It should be noted that this is only for further improvements in case more than one transmitter is available. TagFi works properly with a single pair of WiFi transmitter and receiver.

Algorithm 1: TagFi Localization Algorithm

Data: CSI Measurement at the WiFi receiver

Result: Location of the tag

initialization;

for each packet $i \in 1, 2, \dots, P$ **do**

- Sanitize CSI phase response from offsets using procedure in [42].
- Append the vectorized CSI to measurement matrix X as in Equation 7.

end

Compute signal eigen values E_s of XX^H

for paths $i \in 1, 2, \dots, L$ **do**

- Calculate the orthogonal projection of $i - 1$ estimated paths $P_A = 1 - A(A^H A)^{-1} A^H$, $A = [A_1, \dots, A_{i-1}]$ where, $A(\theta, \varphi, \tau)$ is the steering vector of estimated paths with AoA θ , AoD φ , and rToF τ with unit attenuation.
- Evaluate RAP-MUSIC spectrum $\operatorname{subcorr}(E'_s, A') = \frac{(A')^H E'_s (E'_s)^H A'}{A' (A')^H}$, where $E'_s = E_s P_A$, $A' = P_A A$
- Obtain AoA, AoD, rToF of multipath component i as $\operatorname{argmax}(\operatorname{subcorr})$
- Append the steering vector of the new paths A_i to A

end

- Declare the direct path between WiFi transceivers as the path with shortest rToF
 - Cluster AoAs and AoD, from multiple packets of the remaining resolved peaks
 - Select the cluster with highest probability density as the backscatter path
 - Minimize objective in Equation 14 and solve for the tag's x, y location relative to the WiFi receiver.
-

3.5 TagFi PHY Design

Each tag has a unique modulation code consisting of a balanced sequence of 0s and 1s that defines when to toggle the switch's impedance. The tag periodically switches the internal impedance using this code and a fixed

period to stay in each state. TagFi identifies each tag by decoding the received backscatter signal. To extract this modulation code, TagFi first computes the steering vector $\vec{a}(\theta_b, \varphi_b)$ corresponding to the tag's reflection path. The steering vector defines the expected phase shifts across the transmitting and receiving antenna arrays, given the tag's AoA and AoD extracted in the previous steps. Then, it finds the tag's state during each packet by computing the correlation of the tag's steering vector with the CSI of every packet in a sequence. We expect this correlation to be higher for packets with the tag in reflective mode since the corresponding steering vector is contained within the signal subspace. As such, we define a thresholding mechanism on the following correlation function

$$Corr_p = \left\| \vec{a}(\theta_b, \varphi_b) \times \vec{H}^p \right\|, p = [1, 2, \dots, P] \quad (15)$$

where \vec{H}^p is the CSI of the p^{th} packet. If $Corr_p$ is greater than $Tres_c$, the modulation mode (or the code bit) is determined as 1 (or reflective) for that packet and 0 (or non-reflective) otherwise. We define threshold $Tres_c$ to be $\mu \pm \sigma$, where μ and σ are the mean and standard deviation of $Corr_p$ across the P packets. To filter out the noisy estimates, the correlations that fall between $\mu - \sigma$ and $\mu + \sigma$ are ignored.

However, the extracted code bits do not map directly to the tag's ID. First of all, the WiFi network is known for its bursty behavior, so the number of WiFi packets affected by each modulation state will be different over time. Second, there is no synchronization between the tag modulation and WiFi devices, so we don't know at what position the sequence becomes periodic. To address these challenges, TagFi first uses the timestamp information from the packet header to define the relative position of the code bits. Then, it temporally localizes the edges by looking at the differential between sequential code bits. As shown in Figure 8, TagFi divides the period between two sequential edges by the expected modulation period to calculate the modulation sequence. As mentioned before, the duration that the tag stays in one mode (known as modulation period) is adapted to the packet rate of the WiFi network and is known to the WiFi receiver. Finally, TagFi searches for a periodic code of known length to find the tag's ID.

3.6 TagFi MAC Design

Existing WiFi backscatter systems implement MAC-layer techniques and wake-up procedures for supporting multiple access as well as handshaking with the tag to initiate backscattering. However, in the presence of a wake-up protocol, the WiFi transmitter (e.g the WiFi access point), the receiver (the user's handheld device) and the tag need to coordinate together and synchronize the procedure. However, this is not going to be compatible with current WiFi infrastructure and requires modification in the pre-existing WiFi access points. To address this issue, we adapt a fully asynchronous model, in which the tag is blindly backscattering the ambient WiFi traffic in favor of simple and ultra-low power tag design. Then, the WiFi receiver sniffs packets transmitted from any WiFi access point or other devices in the room and analyzes the signal locally to extract the piggybacked tag reflection on top of ongoing WiFi packets.

However, such asynchronous protocol requires the tag to constantly perform the switching, which could potentially drain battery faster in long term. TagFi uses two tricks to avoid this potential issue. First, TagFi's tag adapts a slow switching rate at the expense of longer scan time. The intuition is that RF switches usually have extremely low static power consumption and only draw significant power when changing the state. So, the WiFi receiver, which is fully powered, can scan for a longer period to capture enough samples for tag detection and localization. Our empirical analyses based on the average size of packets and the WiFi packet rate show that a minimum modulation period of $5ms$ (equal to modulation rate of $200Hz$) provides the best performance in practice. More detailed analysis on tag's power consumption is provided in Section 4.2. In addition, to further reduce the power consumption as well as scaling TagFi to multi-tag scenarios, we adapt a pulse-width modulation (PWM) for our coding scheme, in which each tag selects a modulation frequency that corresponds to different number of consecutive 0s and 1s (as shown in Figure 9a). This essentially reduces the number of switch toggling

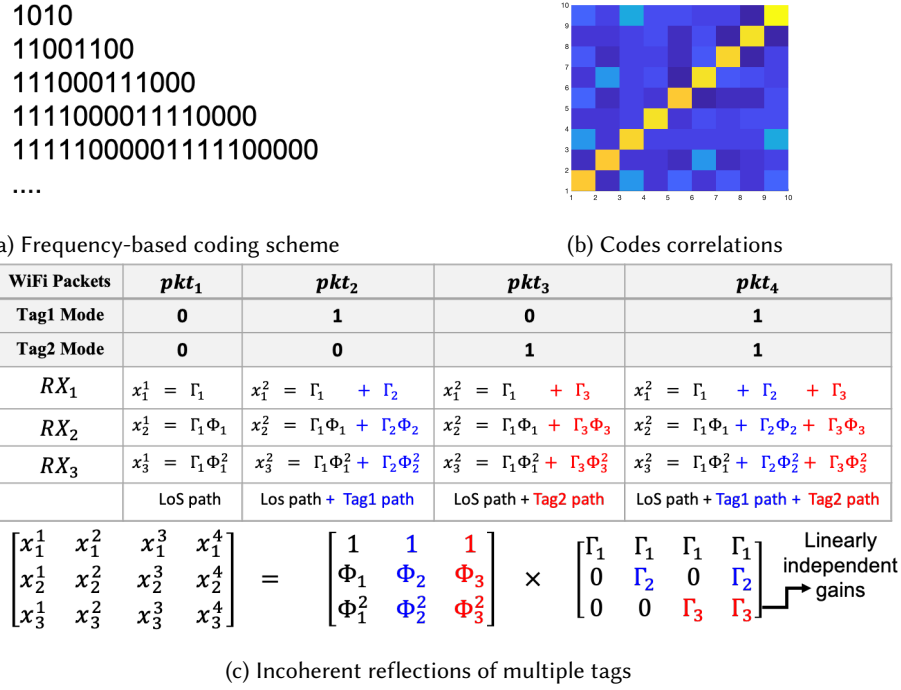


Fig. 9. TagFi leverages a (a) frequency-based coding scheme. (b) The low cross correlation of the codes and (c) the resulting incoherent reflections enables TagFi to differentiate multiple active tags from each other.

at the tag specially at longer code lengths, while providing low cross-correlation between different tags (Figure 9b). In the next section, we discuss how this coding scheme affects the localization delay in multi-tag scenarios.

3.7 Concurrent Operation

TagFi’s asynchronous architecture supports both multiple tag and multiple reader operations at the expense of slightly higher delay in localization.

Multiple Tags: One of the important improvements of TagFi over conventional RFID or WiFi-based localization systems is its potential to localize multiple tags simultaneously. The key intuition is that the backscatter signals of different modulations not only are incoherent with the other multipath signals, but also incoherent with each other. So, by assigning unique modulation schemes to each tag, we can separate their reflections from each other even when operating concurrently. While there are different coding schemes that can be used here (e.g. Gold codes, PN codes, etc), we define the ID of each code based on their switching rate as shown in Figure 9a. In this scheme, the period of each bit is fixed and common between all tags (here defined as 5 ms) and the switching rate is controlled by the number of consecutive 1s and 0s. The low cross-correlation of the codes (shown in Figure 9b) allows us to distinguish reflections from concurrently active tags even without synchronization. To better explain this capability, let’s say there are two active tags with the modulations of 1010 and 11001100, where “1” means the tag is in the reflective mode and “0” indicates the non-reflective mode. Without loss of generality, let us assume there is only the line-of-sight path and the backscatter signals from the tag. As shown in Figure 9c, different modulation modes of the two tags create different signal superpositions across packets with linearly independent coefficient gains, thus resulting in incoherent paths.

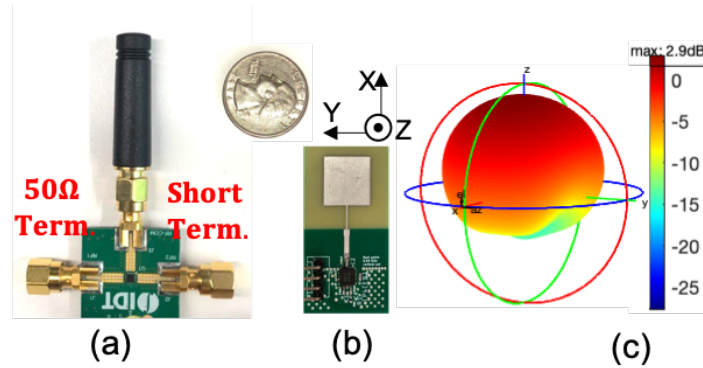


Fig. 10. Two prototypes of TagFi's tag (a) using off-the-shelf components, and (b) a custom design with (c) the radiation pattern of the on-board PCB antenna.

Even though such semi-orthogonal codes provide the desired separation between different tags, the code length is linearly proportional to the number of active tags, which could result in increasing delay in localization. To provide a ballpark estimate of this delay, let us consider 10 active tags in the vicinity of a WiFi receiver. We require 20 bits to define 10 unique orthogonal codes, representing each tag's ID and let's consider five repetitions of the code for mobile path filtration (explained in Section 3.3.2). So, the receiver's scan time for localizing 10 tags will be on the order of $5ms(\text{mod period}) \times 20(\text{code len}) \times 5(\text{code rep}) = 0.5$ seconds. It should be noted that the tag identification resolution is also dependent to the receiver's multipath resolution capabilities. Given the number of antennas and subcarriers available in commodity WiFi devices, our empirical studies show that TagFi requires at least 20-50 cm distance separation between tags to be able to distinguish them from each other. This effect is further studied in Sec. 5.4.

Multiple Readers can co-exist: In our setup, any WiFi-enabled device that is equipped with multiple antennas can act as the reader – each perhaps serving different applications. With recent developments in MIMO communication, most personal devices including laptops, tablets, and even some smartphone models are equipped with multiple antennas. In addition, given the inherent shared medium of wireless channels, any WiFi receiver in the vicinity of the access point can sniff and collect the broadcasting packets and estimate the CSI matrices. Each device can operate independently and locally, computing the location of the tags. We note that our system can piggyback on pre-existing WiFi traffic in the network without necessarily injecting new traffic or any communication overhead. Our system also does not affect the reception quality of ongoing WiFi transmissions, since reflections from TagFi tags can effectively be modeled as signal multipath – much like reflections from other surfaces (e.g. walls, furniture) that are automatically compensated for by WiFi receivers.

4 EVALUATION

4.1 Prototype Implementation

We developed multiple prototypes of the WiFi tag, shown in Figure 10. Our first design uses off-the-shelf components such as an IDT-F2977EVBI¹ RF switch evaluation kit that is connected to a 5 GHz WiFi antenna, a 50Ω termination and a short circuit termination to emulate “reflective/non-reflective” states. It should be noted that the tag does not need a WiFi transceiver as it passively backscatters the available WiFi signals. Next, we

¹<https://www.idt.com/document/dst/f2977-datasheet-rev-o>

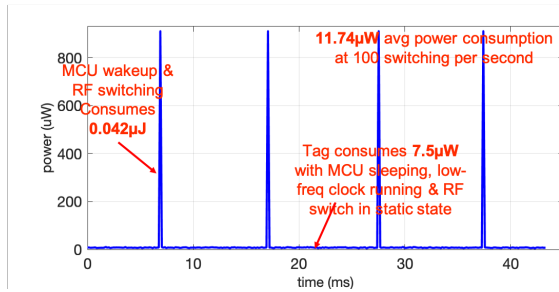


Fig. 11. TagFi’s tag consumes an average power of $11.74\mu W$ at 100Hz switching rate.

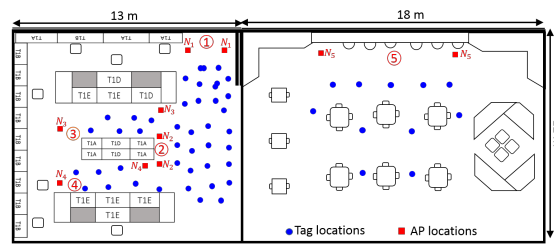


Fig. 12. Experimental Setup

prototype the on-board antenna design and RF circuitry using a high-isolation Analog Devices HMC849ALP4CERF RF switch². The antenna is designed to have high gain on 5GHz WiFi band. The gain pattern of the antenna (Figure 10-C) shows that it has a uniform directivity over the upper hemisphere. In our final prototype, we focus on lowering power consumption while maintaining similar detection performance. This tag design uses a CEL CG2415 low-power RF switch³ and a TI MSP430G2210 low-power microcontroller⁴ (MCU) to control the switch. This MCU does not use an external oscillator and can thus save significant power while maintaining RAM and peripheral states as the MCU core is sleeping.

Our WiFi transmitter and receiver are Intel NUCs equipped with Intel 5300 NIC. We install Linux 802.11n CSI tool [16] in the receiver to collect CSI measurements from 3-element antenna arrays at each of the WiFi transmitter and receiver, and 30 frequency subcarriers. Devices are set to work in monitor mode using channel 128 at 5.63 GHz frequency with a 40 MHz bandwidth, and MIMO-OFDM spatial multiplexing mode. The transmission rate of packets is set to 3000 Hz .

4.2 Tag Power Consumption

The CEL CG2415 RF switch in our final tag prototype was selected for its power and ability to function at 6 GHz. A power trace from this prototype was captured on a Keysight DC power analyzer and is shown in Fig. 11. Both the MCU and the RF switch in this design have extremely low static power consumption i.e. the tag only draws significant power when the MCU has to wake up, process the next state and change the state of the RF switch. Normally, the MCU remains in a low-power sleep mode with an internal low-power low-frequency oscillator running (LPM3) and the RF switch maintaining it’s reflective or non-reflective state. Periodically, an interrupt will fire on the MCU indicating that it is time to change the state of the RF switch. The entire process of waking up the MCU, computing the next tag state and changing the state of the RF switch takes around $50\ \mu\text{s}$ and consumes $0.042\ \mu\text{J}$ of energy per switching cycle. Thus, the overall power consumption of the tag is dependent on the number of switch state changes. For a rate of 25, 50, 100, 200 state changes per sec, we end up with an amortized power consumption of 8.5, 9.6, 11.7 and $16.0\ \mu\text{W}$. We estimate that this tag could operate on a 3V CR2032 lithium coin cell for 6.7, 6.0, 4.9, 3.6 years respectively, assuming an efficiency of 75 %. Alternatively, this amount of power can easily be supplied by a number of energy harvesting systems in existing literature. A well-placed bank of bypass capacitors would deal with any problems that might occur in the energy harvesting

²<https://www.analog.com/en/products/hmc849a.html>

³<http://www.cel.com/pdf/datasheets/CG2415M6.pdf>

⁴<http://www.ti.com/product/MSP430G2210>

system due to the 1 mW peak power consumption. We should note that the energy harvesting implementation is outside of the scope of this paper.

4.3 Experimental Setup

We deploy our system in a regular office building that spans an area of $12 \times 30m$, as illustrated in Figure 12, in the presence of 1-5 occupants and a lot of furniture and electrical equipment with rich multipath propagation. We place the transmitter-receiver pair in 5 different locations, shown in Figure 12, and place the tag in random locations for a total of 51 test spots. In addition, for any tested location in Figure 12, we collect CSI measurements in both directions and estimate the location of the tag for both communication directions, which results in a total of 102 different experimental scenarios. In each experiment, 1000 packets are transmitted with a 3ms time interval and the tag modulates constantly using 1010 code with the rate of 100Hz. The main results are calculated based on the sequences of 10 modulated packets (time window of 30ms) and the impact of the number of packets on localization is discussed in Section 5.3.

We obtain the ground truth AoA, AoD, and tag locations with a combination of laser range finder and construction protractor as well as an Aruco-marker and camera for mobile experiments. Note that the previous WiFi-based tag localization systems either use frequency shifting [24], or require specialized WiFi helpers to communicate with the tag [57], none of which is compatible with our setup. Instead, we compare TagFi with MonoLoco [42], which is the state-of-the-art single-point localization system based on active WiFi radios. In MonoLoco, the target is equipped with an active WiFi transmitter instead of a passive tag as in TagFi. Therefore, the localization algorithm is estimating the direct path parameters instead of the reflection. However, this technique is closest to our algorithm in terms of only requiring a single receiver with no triangulation or coordination between multiple anchor points. We also compare the performance of TagFi under two situations: when (1) the distance between the WiFi AP and the WiFi receiver is known (such as scenarios where two APs or one AP and a fixed WiFi device in the room are used for localization), and (2) the distance of the AP and WiFi receiver is unknown (such as when the handheld devices are used to find the object of interest in a new environment).

4.4 Evaluation Overview

We deployed TagFi at different locations in various rich-multipath environments. Here is a summary of the main results from the evaluation.

- TagFi achieves similar localization accuracy as MonoLoco, which requires an active WiFi radio at the object of interest. TagFi's median localization error is 30cm without requiring an active radio at the tag, by only using a single WiFi receiver and without knowing the relative distance of the WiFi transmitter and receiver.
- TagFi is capable of localizing multiple tags simultaneously with minimal performance degradation as opposed to the time-multiplexing mechanism used in RFID or other WiFi backscattering systems. For cases with close-by tags, the median localization accuracy drops to 43cm with a 90th percentile below 1m. A snapshot of multi-tag localization performance is shown in Figure 2c.
- In challenging conditions such as a dynamic environment where the tag is blocked from the WiFi reader or in the case of a mobile device, TagFi's performance does degrade, however, it still provides useful localization accuracy within 0.7 to 0.95m. Such errors can be compensated by integrating measurements over time as shown in Figure 21a.
- Compatibility of TagFi with commodity WiFi devices as well as its single-point localization capabilities enable a ubiquitous and deployable platform for object tracking and localization with AR-enhanced visualization (shown in Figure 2b).

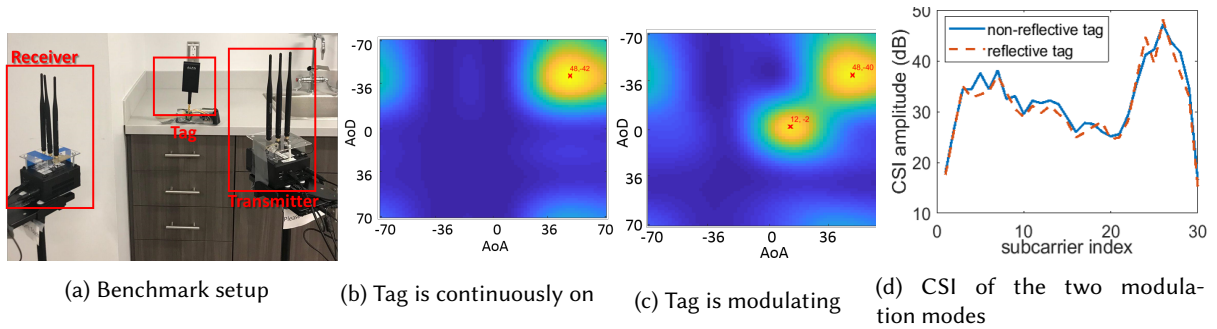


Fig. 13. Benchmark experiments. The tag reflection with AoA and AoD of 0° is only detectable when the tag starts modulating the WiFi packets by switching between reflective/non-reflective modes. This is despite the fact that no obvious variation can be observed in the raw CSI values as the tag modulation changes.

4.5 Benchmark Verification

We first verify the key innovation of TagFi, which is utilizing path modulation for eliminating the coherence of the backscatter signal with other multipath reflections. We place a pair of WiFi transceivers in an empty environment at proximity of 1 meter to each other, shown in Figure 13a. The tag is equipped with a 10 dBi directional antenna⁵, to enforce a stronger reflection for better visualization, and is placed between the transmitter and receiver in a position that creates a backscatter path with AoA and AoD of 0° for verification. First, we switch the tag into “reflective” mode, so a backscattered path is expected from the transmitter to the tag to the receiver. However, we can see in Figure 13b that only one cluster of AoA-AoDs is obtained, which corresponds to the strong LoS path between the transmitter and receiver. The tag’s reflection is not detected in this case due to significant attenuation.

Next, the tag modulates the backscatter signal by continuously switching the antenna between reflective and non-reflective modes. We can see in Figure 13c that two clusters of AoA-AoDs are derived in this case: one belongs to the LoS path and the other belongs to the backscatter path. The AoA and AoD of the new derived path are clustered at 0° , matching the angles of the tag. This confirms the mathematical formulations presented in Section 3.1 and the expected rank increase in the system of equations due to the backscatter modulation. Finally, Figure 13d demonstrates that this approach effectively detects the tag reflection even though there is no obvious change in the raw CSI values as the tag switches the modulation mode. This confirms the importance of this realization and the significant improvement over the state-of-the-art WiFi backscattering techniques [21] that rely on the changes of the raw CSI amplitude to extract the modulated information.

4.6 Tag Localization Accuracy

We evaluate TagFi localization accuracy by deploying the system in two spaces of $12 \times 13m$ and $12 \times 18m$ with rich multipath propagation that replicates the scenarios used for evaluation of state-of-the-art systems like [5]. It should be noted that the experiments of this paper are conducted in the presence of moving people, which confirms the robustness of TagFi in dynamic environments. We first place the tag at each of the tested locations shown in Figure 12. we also vary the location of the TX-RX link throughout the evaluation area between locations 1-5. For each tag location shown in blue, the closest TX-RX link localizes the tag. Since the detection range of the tag is constrained by the power of the backscattered signal, we discard instances where the tag does not respond and will analyze the tag detection rate later in Section 4.7.

⁵Alfa APA-M25 dual band 2.4GHz/5GHz 10dBi high gain directional indoor panel antenna with RP-SMA connector

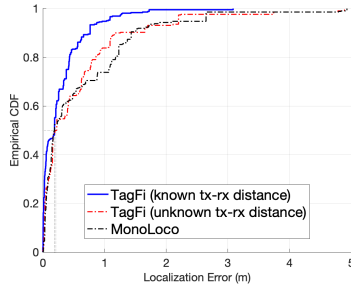


Fig. 14. TagFi can achieve median error of 17 and 30 cm in tag localization with and without knowing the WiFi transmitter’s location, respectively.

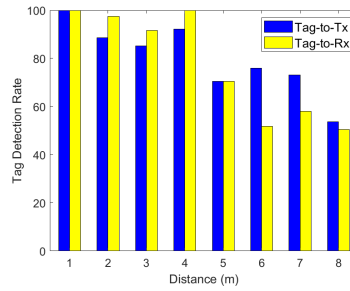


Fig. 15. The detection rate decreases from 100% in 1m to 50% in 8m distance from the links.

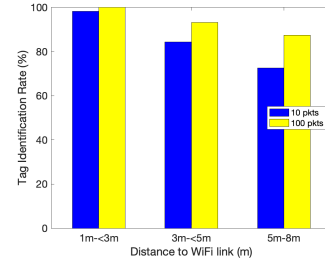
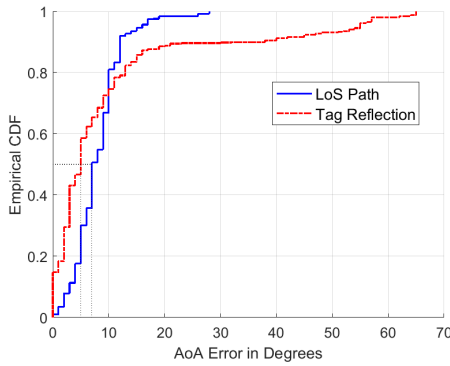
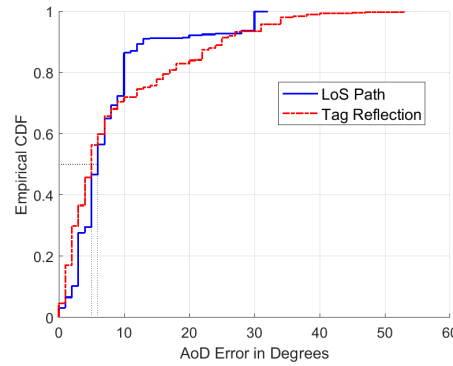


Fig. 16. TagFi identifies the tag modulation code with 100% accuracy in 1-3m to 80% in 5-8m.



(a)



(b)

Fig. 17. The high performance of TagFi in tag localization is the result of the high-resolution AoA and AoD estimations.

Figure 14 shows the CDF of TagFi’s localization error in two cases: (1) the location of the transmitter is known to WiFi receiver or estimated using a separate localization system (2) the WiFi receiver jointly localizes both the tag and WiFi transmitter using multipath triangulation [42]. TagFi can achieve a median error of 17cm and 30cm, as well as 80th percentile errors of 62cm and 1.3m in cases 1 and 2, respectively. As expected, the localization error of transmitter adds to the error of the tag location system. However, these results are comparable to state-of-the-art WiFi-based tag localization systems that use multiple APs and frequency shifting [5, 24]. In addition, TagFi’s localization performance is comparable with MonoLoco that uses an active WiFi transmitter at the target. Theoretically, MonoLoco should have achieved higher accuracy because the signal to noise ratio of the signal from an active transmitter is much higher than a passive backscatter tag. However, Monoloco uses an arbitrary reflection in the environment combined with the direct path to achieve single-point localization, as opposed to TagFi which leverages the reflection from tag with known modulation pattern. So this allows TagFi to achieve a similar performance as MonoLoco in similar setups. In addition, the primary reason behind the high performance of TagFi is its ability to separate the backscatter signal from multipath interferences. Generally, the tag localization accuracy depends on several factors including the profile of multipath propagation, the distance from WiFi link, and the presence of obstacles, which are studied in the next sections.

4.7 Tag Detection Range

To test the working range of TagFi, we first fix the tag-to-TX distance at $0.7m$, while varying the tag-to-RX distance, and vice versa. Figure 15 shows the tag detection rate with respect to its distance from the WiFi transmitter and receiver. As the tag moves away from the WiFi transmitter, the detection rate decreases from 100% in $1m$ to 53% in $8m$ distance. Similarly, as the tag moves away from the WiFi receiver, the tag detection rate decreases from 100% to 50% in $1m$ and $8m$ distances, respectively. Theoretically, the power loss of a radio signal is proportional to the inverse square of the distance, so as the length of the backscattered signal increases, it undergoes more attenuation and a smaller fraction of the signal arrives at the receiver along the backscatter path. In general, TagFi has smaller localization range compared to frequency shifting tags due to higher in-band interference between the backscatter signal and the LoS path. We consciously sacrifice range to improve ease of deployment and practicality of the localization system.

We can also see that the detectability of the tag is more sensitive to the tag's proximity from the WiFi receiver, so we can ensure high detection performance by maintaining a clean direct path between the tag and the WiFi receiver. This requirement can be fairly satisfied in regular office buildings, considering that there are usually multiple WiFi devices locating in different rooms. In addition, TagFi only requires a single WiFi receiver to locate the tag with no additional coordination with any other devices. So to locate a tag in practice, the smart building controller will inquiry all WiFi devices, they independently eavesdrop the transmitted packets and apply TagFi. So, we can expect that the WiFi device in the vicinity of the tag to accurately locate it, which compensates for the limited range of the system.

We also evaluate the performance of TagFi in extracting the tag's modulation code. As shown in Figure 16, the tag identification accuracy starts from 100% in ranges between 1-3m and degrades to 80% for ranges as large as 5 to 8 meters.

5 SENSITIVITY ANALYSIS

5.1 AoA-AoD Estimation Accuracy

We measure the accuracy of AoA and AoD estimations using the absolute difference between the ground truth and estimated values for both the backscatter path and the LoS path between WiFi transceivers. Figure 17a shows the CDF of the AoA estimation errors. TagFi can achieve median errors of 7° and 5° and 80^{th} percentile of 10° and 13° for the LoS and backscatter paths, respectively. In addition, Figure 17b shows the performance of AoD estimations, for which TagFi achieves median accuracy of 6° and 5° for the LoS and backscatter paths, respectively. The 80^{th} percentile accuracy of AoD estimations degrades to 10° and 18° . These results are comparable to WiTag's performance [24], which also reports a median accuracy of 7° to 14° in AoA estimation. The key point is that TagFi achieves similar accuracy without requiring to shift the frequency of backscatter signal or a high-power circuitry in the tag.

As can be seen in Figure 17, the LoS estimates in both the AoA and AoD CDFs have shorter tails compared to the ones for the backscatter path. Since a higher signal power propagates along the LoS path, the angular estimates are more accurate for this path. Another factor affecting the performance of super-resolution algorithms is the direction of the incident signals. We expect a higher estimation error is expected as the incident angle of the signal approaches the angle of the array. For example, when the direction of the backscatter signal is close to 90° , it is hard to identify the direction since similar phase differences will be introduced across the antennas for both $90^\circ - \epsilon$ and $-90^\circ + \epsilon$ for $0^\circ \leq \epsilon \leq 20^\circ$. In our current experiments, the majority of the tag positions (78%) create a backscattered signal at AoAs or AoDs larger than 40° , which results in a higher super-resolution error for the backscatter signal. This though is a limitation of the linear antenna arrays and can be addressed by using circular antenna arrays in future extensions of TagFi. Finally, the relative angle between the LoS path and the tag reflection can affect TagFi's performance. The smaller this relative angle is, the higher localization error

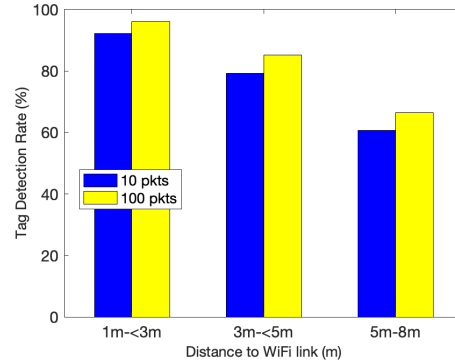
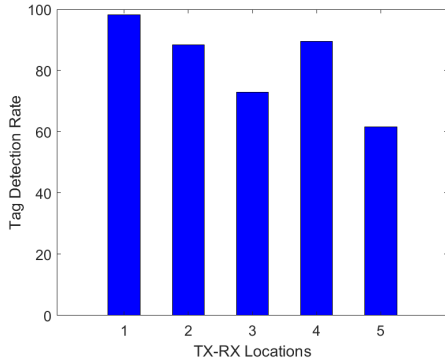


Fig. 18. Tag detection rate for different TX-RX locations. Fig. 19. Tag range improves by integrating more packets.

is expected as it is limited by the angular resolution of the super-resolution algorithm as well as the narrow geometry of the multipath triangle created by the two paths. However, our analyses show that TagFi still achieves $0.73m$ localization accuracy even when the relative angle of the two paths are as small as 10 degree. This can be further improved as the user walks around the space, creating different multipath triangles.

5.2 Impact of TX-RX Location

Next, we evaluate the effects of the WiFi link location on detecting the tag's backscatter signal. In each location, we place the WiFi transmitter and receiver such that they are 0.7 to $6m$ away from each other. The WiFi link locations are shown as 1-5 in Figure 12. For each tag location shown in blue, the closest TX-RX link to the tag performs the localization. We see in Figure 18 that the probability of detecting the tag is changing from 98% in location 1 to 60% for location 5. The main factors affecting these variations are a combination of destructive/constructive interference and the distance of the tag from the WiFi link. For example, in locations 3 and 4, the tag is located between cluttered tables and multiple electronic and metallic items, creating rich multipath propagation, which results in lower detection rate. In addition, in location 5, the tag is located in longer ranges from the WiFi transmitter and receiver, for which the strong LoS path between the WiFi transmitter and receiver swamps the backscatter signal, making the tag detection more challenging. In more practical setups, the user can walk around with the WiFi receiver to collect more spatially diverse measurements over time.

5.3 Effect of Number of Modulated Packets

TagFi primarily relies on the modulation of the tag reflection to identify this weak backscatter signal from complex multipath propagations. So, receiving WiFi packets with different modulation modes is critical for achieving high accuracy in tag localization. Figure 19 measures the tag detection rate for different number of packets grouped based on the Euclidean distance of the estimated tag and tx-rx link. Utilizing more packets improves the range by filtering the noise in measurements. However, our analyses show that the number of packets has minimal impact on localization accuracy, which means our adapted super-resolution algorithm can accurately extract the geometry of the tag as long as the backscatter signal is above the noise floor.

5.4 Multi-tag Performance

TagFi asynchronous MAC protocol allows the WiFi receiver to localize multiple tags at the same time. We evaluate this by placing three different tags in a small indoor space in different ranges from each other (from 20cm to

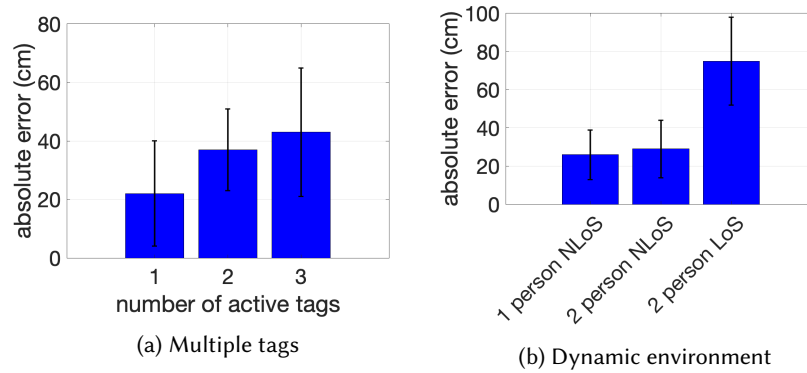


Fig. 20. TagFi can robustly identify and locate multiple active tags, even in dynamic and multipath-rich environments.

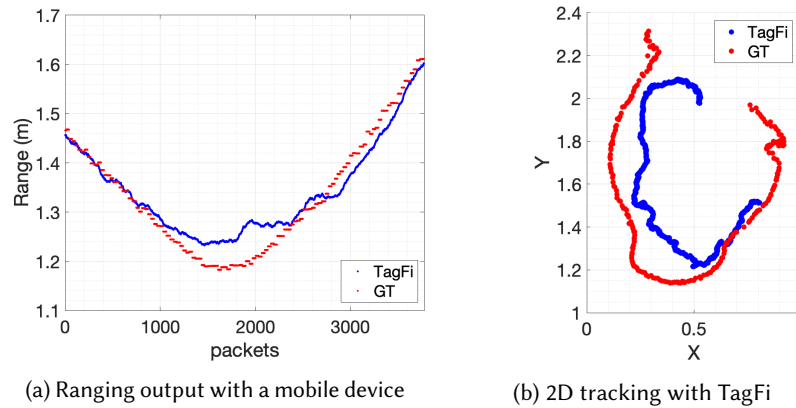


Fig. 21. Snapshots of TagFi’s localization output used in tracking applications.

1m). We vary the number of active tags from 1 to 3. In all of these experiments, the transmitter and receiver where 5m apart in two corners of the room (showed in Figure 2a). A snapshot of the tags locations is shown in Figure 2c. In each experiment, we look for any number of active tags in the collected data and estimate the location of the detected tags. Figure 20a shows the median localization accuracy in each of these setups. We see that the accuracy slightly reduces from 20cm to 43cm when 3 tags are active. We found that most of the errors with additional tags occur when they are co-located and hence very close to each other. This is due to the limited aperture of WiFi devices in resolving nearby paths. This can be addressed by using signal measurements from multiple locations (when the user slightly moves the WiFi receiver) or through tracking approaches (an additional layer that could be done as future work). It should be noted that TagFi can simultaneously estimate the relative location of the WiFi receiver with respect to the AP as well as the location of the tag with respect to the WiFi receiver (leveraging Multipath Triangulation [42]). This demonstrates that we can localize without needing to know the distance between the WiFi receiver and the AP.

5.5 Impact of Mobility

The single-point localization capabilities of TagFi makes it a perfect object localization approach in any arbitrary environments that may not have a localization infrastructure in place (e.g. public and shared places such as hotels, restaurants, AirBnB, and guest homes). The user only requires a personal WiFi device like a tablet or laptop associated with the access point in the building and a tag attached to their objects of interest. However, robustness of TagFi against various multipaths and mobility scenarios is essential for such applications. So, we evaluated the performance of TagFi in different mobility scenarios including different environment dynamics with moving people creating various multipaths as well as mobility of the WiFi receiver itself.

5.5.1 Dynamic Environment. We conducted indoor experiments in a rich-multipath environment when the tag is approximately 5m away from the WiFi receiver and have one or two people walking very close to tag and sometimes blocking the LoS. As shown in Figure 20b, we notice negligible impact on TagFi's localization performance even in such mobility scenarios. However, the tag is missed a few times in the blockage scenarios as the reception of the direct path is essential for detecting and locating the tag. However, such missed detections can be easily handled by integrating measurements across multiple packets in more crowded areas. To show this, we used 100 packets instead of 10 packets in the experiment with 2 people walking in the LoS. The average localization accuracy improved from 78cm to 41cm, showing the effectiveness of larger time integration in highly dynamic environments. This is mainly due to the clustering techniques defined in Section 3.3.2 for differentiating tag reflection from mobile paths.

5.5.2 Mobile WiFi Devices. Next, we evaluated the performance of TagFi for a mobile client such as when a user locates an object from her handheld devices such as tablet or laptop. We perform several experiments while the tag and WiFi access points are fixed and the WiFi receiver walks toward the tag, walks away, or moves randomly in the space. To calculate the ground truth, we use a camera co-located with the WiFi receiver and an Aruco-marker co-located with the tag. We see that TagFi can achieve an average accuracy of 17cm with 90th percentile of 61cm even with a mobile client as a result of tag's high switching rate (every 5ms) compared to the typical walking velocity. Figure 21a depicts a snapshot of user's walking trace and range estimates compared with the ground truth and Figure 21b shows the 2D tracking capability of TagFi in mobile scenarios.

5.6 Effect of Interfering WiFi Traffic

In spite of the previous backscattering systems such as RFID that rely on a sequence of handshaking protocol between the tag and the reader, TagFi performs localization by double purposing the on-going data packets. This is specifically possible since any commodity WiFi receiver can collect CSI data by just sniffing the broadcasting packets from an AP. In addition, the asynchronous MAC protocol of TagFi allows the WiFi receiver to locate the tag without requiring any explicit coordination between the tag and WiFi transceivers, injecting any new traffic or any communication overhead. In addition, TagFi does not affect the reception quality of ongoing WiFi transmission, since tag reflection can effective be modeled as a multipath signal similar to reflections from other surfaces such as walls or furniture. We evaluated this effect by comparing the average packet loss of our network when the tag is on and off. Our analyses show that 99.3% of the packets transmitted in the conducted experiments has been received properly during the tag modulation. This is comparable to the packet delivery rate of our wireless network without an active tag (99.4%). This is mainly because the tag reflection is considerably weaker than the typical indoor multipaths. As shown in Figure 13d, the modulation of the backscatter signal has minimal impact on the raw CSI values so it does not really interfere with existing WiFi traffic.

6 APPLICATIONS

TagFi's core advantage is its ease of deployability and compatibility with pre-existing WiFi infrastructure. Any WiFi device that is equipped with multiple antennas can be converted to a tag reader without requiring new localization infrastructure in place. Contrast this with state-of-the-art RFID-based localization solutions that require expensive and complex sensor deployment, or Bluetooth-based solutions that require frequent battery exchange. In terms of versatility, the numerous applications of RFID localization also apply to TagFi, with TagFi having the added benefit of running on pre-existing WiFi infrastructure. This leads a new paradigm of converting commodity WiFi devices into sensing hubs can enable rapidly deployable IoT sensing applications. Some of these applications are presented as follows.

Object Finding in Arbitrary Environments: The aforementioned features of TagFi allows us to build a ubiquitous localization ecosystem for any object, powered or battery-free, with or without WiFi radios, and in any arbitrary environment such as hotels, restaurants, or AirBnBs with no pre-installed localization infrastructure. So, if the occupants are looking for an object (e.g. keys, toys, tools, etc), they can just use their personal WiFi devices paired with the access point in the room to find and locate it relative to their personal device, without requiring any extra information such as the layout of the building or the location of the WiFi access point in the room. TagFi enables such an automated ecosystem with only software updates in all devices involved and minimal deployment effort.

Augmented Reality: TagFi is a natural fit to improve context-awareness for augmented reality. Several AR helmets are already WiFi enabled and can therefore serve as WiFi access points to search for TagFi tags in the environment. These could serve as beacons for calibration or object tagging, much akin to how April Tags are used today [49], with the added advantage of not requiring the tag to be in direct field-of-view of the AR helmet.

Tracking Wearables and the Body: Similar to RFID, different interference algorithms can be built on top of TagFi's object tracking and localization. When tracking wearable devices equipped with TagFi tags, one can enable applications ranging from behavioral monitoring, activity or gesture recognition, fall detection in elderly monitoring, etc. TagFi's ability to perform single-point localization and compatibility with commodity WiFi devices, allows us to enable such services in any environment without pre-installed sensing infrastructure.

7 DISCUSSION

In this section, we discuss future extensions of TagFi and mechanisms to relax assumptions made in our current implementation of the system.

Operating range: In our current implementation, we show that TagFi can operate up to ranges of 6-8 m, while achieving sub-meter accuracy. However, some applications such as asset tracking in industrial contexts may require longer range operations and higher resolution, especially in dense deployments. This paper provides a proof of concept deployment for seamless WiFi backscatter localization and there are several potential avenues for range and resolution improvement in future work. Specifically, our work can naturally benefit from recent advances and emerging technologies in wireless systems (e.g. 802.11ac, WiFi 6, larger antenna arrays, and massive MIMO). These remain fully compatible with our architecture and can result in higher accuracy and resolution owing to their larger bandwidth (e.g. 160MHz in 802.11ac), higher sampling rate, and larger number of antennas available. In addition, the operating range of the tag can be improved by increasing the radar-cross section (RCS) of the tag's antenna and the differential RCS between the two states of the tag. We believe this can be achieved with innovations on the antenna design and low-loss RF circuitry at the tag.

3D Localization: TagFi currently localizes the tag in the 2D space. This is a theoretical limitation of single-point localization systems with planer antenna arrays (e.g. TagFi or MonoLoco). However, by relaxing one of these two assumptions, 3D localization can be achieved such as leveraging triangulation between multiple receivers,

3D antenna arrays at the WiFi receiver, or leveraging the motion of the tag/WiFi receiver. However, for our application set (finding and searching for objects of interest), 2D localization is still useful to provide room-level localization.

Impact of Blockage: TagFi assumes a direct path from the WiFi transmitter to the tag to the WiFi receiver. As a result, the performance of TagFi degrades in the case of complete tag blockage. However, we see in Section 5.5.1 that temporary blockages due to human motion or environment dynamics can be compensated by combining temporal estimates. This is a long-standing challenge in object localization systems which share this limitation and localizing tags under complete blockage of the direct reflection continues to be an open problem.

Robustness to Certain Orientations: The current implementation of TagFi assumes linearly polarized antennas on the WiFi transceivers and the tag, so detecting the tag reflection at certain orientations are more challenging. However, this can be simply addressed by adapting a circularly polarized antenna at the tag without requiring any modification on the localization algorithm. We leave this extension and a thorough study of free tag motion in 3D space for future work.

High Mobility: We evaluate our system on different mobility scenarios such as a highly dynamic environment with various mobile users as well as mobile clients as WiFi reader and demonstrate that TagFi is fairly robust in these scenarios. By additional post-processing or tracking techniques such as Particle or Kalman filters, temporal measurements can be better integrated to further improve TagFi for highly mobile scenarios and extend it to other applications such as gesture recognition. It should be noted that such techniques are widely studied in the radio backscatter and RFID domains, and these also apply to our tag design.

Scalability: TagFi requires multiple antennas on both the WiFi transmitter and receiver. In our applications, we assume the WiFi transmitter is the WiFi Access Point inside the room and the WiFi receiver/reader is a WiFi-enabled device, either static or handheld, that is equipped with an antenna array. With the ubiquity of MIMO technology in communication, most of the WiFi devices such as laptops, tablets, smart appliances and even newer models of smart phones do have multiple antennas. However, small devices such as smart watches or certain types of older phones cannot be used as WiFi readers since they typically have only one antenna. Nevertheless, TagFi requires multiple antennas to enable single-point localization and localizing targets from a single vantage point through a single antenna device continues to be an open problem. It should be noted that TagFi is compatible with any array configuration and does not necessarily need a linear antenna array.

In addition, the current coding scheme of the tag is designed for home and personal use cases that cover tens of objects spread in a room-size area. To scale this system to a larger number of closely-spaced tags, for contexts such as asset tracking in warehouses or super-markets, we suggest the use of PN codes at the tag that offers improved collision resilience and scalability, albeit with additional implementation complexity at the tag.

8 CONCLUSION AND FUTURE WORK

This paper presents *TagFi*, a novel WiFi-based tag localization system that leverages the passive wireless reflection from an ultra-low-power tag. The key innovation of TagFi is its unique mechanism to extract the weak tag reflection from complex multipath propagations in indoor environments. TagFi shows that modulating the backscatter path across WiFi packets eliminates the coherence of this signal with other multipaths, enabling super-resolution algorithms to estimate the parameters of the backscatter signal. Unlike frequency-shifting tags, TagFi allows the WiFi transmitter, receiver, and the tag to operate on one common frequency as is typical in WiFi, thus improving the practicality of WiFi backscatter localization. In addition, the proposed asynchronous ultra-low power architecture of TagFi can be applied beyond WiFi. In our future work, we plan to scale TagFi to higher frequency ranges and ultra wideband radios.

ACKNOWLEDGMENTS

This research was funded in part by the CONIX Research Center, one of six centers in JUMP, a Semiconductor Research Corporation (SRC) program sponsored by DARPA, and the National Science Foundation (1739333, 1718435, 2030154 and 2007786). We thank our reviewers for their insightful feedback which helped improve this paper. We also thank all members of Microsoft AI and Research, specially Dr. Bodhi Priyantha, for their inputs.

REFERENCES

- [1] 2019. Lost-and-found with Tile tags. <https://www.thetileapp.com/en-us/>.
- [2] 2019. Real-time localization with Decawave tags. <https://www.decawave.com/>.
- [3] Fadel Adib and Dina Katabi. 2013. See through walls with WiFi!. In *Proceedings of the ACM SIGCOMM 2013 conference on SIGCOMM*. 75–86.
- [4] Daniel Arnitz, Klaus Witrisal, and Ulrich Muehlmann. 2009. Multifrequency continuous-wave radar approach to ranging in passive UHF RFID. *IEEE transactions on microwave theory and techniques* 57, 5 (2009), 1398–1405.
- [5] Roshan Ayyalasomayajula, Deepak Vasisht, and Dinesh Bharadia. 2018. BLoc: CSI-based accurate localization for BLE tags. In *Proceedings of the 14th International Conference on emerging Networking EXperiments and Technologies*. ACM, 126–138.
- [6] Salah Azzouzi, Markus Cremer, Uwe Dettmar, Rainer Kronberger, and Thomas Knie. 2011. New measurement results for the localization of uhf rfid transponders using an angle of arrival (aoa) approach. In *2011 IEEE International Conference on RFID*. IEEE, 91–97.
- [7] Paramvir Bahl, Venkata N Padmanabhan, et al. 2000. RADAR: An in-building RF-based user location and tracking system. In *IEEE infocom*, Vol. 2. INSTITUTE OF ELECTRICAL ENGINEERS INC (IEEE), 775–784.
- [8] Dinesh Bharadia, Kiran Raj Joshi, Manikanta Kotaru, and Sachin Katti. 2015. Backfi: High throughput wifi backscatter. *ACM SIGCOMM Computer Communication Review* 45, 4 (2015), 283–296.
- [9] Mathieu Bouet and Aldri L Dos Santos. 2008. RFID tags: Positioning principles and localization techniques. In *2008 1st IFIP Wireless Days*. Ieee, 1–5.
- [10] Kirti Chawla, Christopher McFarland, Gabriel Robins, and Connor Shope. 2013. Real-time RFID localization using RSS. In *2013 International Conference on Localization and GNSS (ICL-GNSS)*. IEEE, 1–6.
- [11] Krishna Chintalapudi, Anand Padmanabha Iyer, and Venkata N Padmanabhan. 2010. Indoor localization without the pain. In *Proceedings of the sixteenth annual international conference on Mobile computing and networking*. ACM, 173–184.
- [12] Brian Ferris, Dieter Fox, and Neil D Lawrence. 2007. WiFi-SLAM Using Gaussian Process Latent Variable Models.. In *IJCAI*, Vol. 7. 2480–2485.
- [13] Jon Gjengset, Jie Xiong, Graeme McPhillips, and Kyle Jamieson. 2014. Phaser: Enabling phased array signal processing on commodity WiFi access points. In *Proceedings of the 20th annual international conference on Mobile computing and networking*. ACM, 153–164.
- [14] Stuart A Golden and Steve S Bateman. 2007. Sensor measurements for Wi-Fi location with emphasis on time-of-arrival ranging. *IEEE Transactions on Mobile Computing* 6, 10 (2007), 1185–1198.
- [15] Abhishek Goswami, Luis E Ortiz, and Samir R Das. 2011. WiGEM: A learning-based approach for indoor localization. In *Proceedings of the Seventh Conference on emerging Networking EXperiments and Technologies*. ACM, 3.
- [16] Daniel Halperin, Wenjun Hu, Anmol Sheth, and David Wetherall. 2011. Predictable 802.11 packet delivery from wireless channel measurements. *ACM SIGCOMM Computer Communication Review* 41, 4 (2011), 159–170.
- [17] Cory Hekimian-Williams, Brandon Grant, Xiuwen Liu, Zhenghao Zhang, and Piyush Kumar. 2010. Accurate localization of RFID tags using phase difference. In *2010 IEEE International Conference on RFID (IEEE RFID 2010)*. IEEE, 89–96.
- [18] Kiran Joshi, Steven Hong, and Sachin Katti. 2013. Pinpoint: Localizing interfering radios. In *Presented as part of the 10th {USENIX} Symposium on Networked Systems Design and Implementation ({NSDI} 13)*. 241–253.
- [19] Avinash Kalyanaraman, Dezhi Hong, Elahe Soltanaghaei, and Kamin Whitehouse. 2017. Forma track: tracking people based on body shape. *Proceedings of the ACM on Interactive, Mobile, Wearable and Ubiquitous Technologies* 1, 3 (2017), 1–21.
- [20] Avinash Kalyanaraman, Elahe Soltanaghaei, and Kamin Whitehouse. 2019. Doorpler: A Radar-based System for Real-Time, Low Power Zone Occupancy Sensing. In *2019 IEEE Real-Time and Embedded Technology and Applications Symposium (RTAS)*. IEEE, 42–53.
- [21] Bryce Kellogg, Aaron Parks, Shyamnath Gollakota, Joshua R Smith, and David Wetherall. 2014. Wi-Fi backscatter: Internet connectivity for RF-powered devices. In *ACM SIGCOMM Computer Communication Review*, Vol. 44. ACM, 607–618.
- [22] Bryce Kellogg, Vamsi Talla, Shyamnath Gollakota, and Joshua R Smith. 2016. Passive wi-fi: Bringing low power to wi-fi transmissions. In *13th {USENIX} Symposium on Networked Systems Design and Implementation ({NSDI} 16)*. 151–164.
- [23] Manikanta Kotaru, Kiran Joshi, Dinesh Bharadia, and Sachin Katti. 2015. Spotfi: Decimeter level localization using wifi. In *ACM SIGCOMM Computer Communication Review*, Vol. 45. ACM, 269–282.
- [24] Manikanta Kotaru, Pengyu Zhang, and Sachin Katti. 2017. Localizing low-power backscatter tags using commodity WiFi. In *Proceedings of the 13th International Conference on emerging Networking EXperiments and Technologies*. ACM, 251–262.

- [25] Rainer Kronberger, Thomas Knie, Roberto Leonardi, Uwe Dettmar, Markus Cremer, and Salah Azzouzi. 2011. UHF RFID localization system based on a phased array antenna. In *2011 IEEE International Symposium on Antennas and Propagation (APSURSI)*. IEEE, 525–528.
- [26] Swarun Kumar, Stephanie Gil, Dina Katabi, and Daniela Rus. 2014. Accurate indoor localization with zero start-up cost. In *Proceedings of the 20th annual international conference on Mobile computing and networking*. ACM, 483–494.
- [27] Steven Lanzisera, David Zats, and Kristofer SJ Pister. 2011. Radio frequency time-of-flight distance measurement for low-cost wireless sensor localization. *IEEE Sensors Journal* 11, 3 (2011), 837–845.
- [28] Xin Li, Yimin Zhang, and Moeness G Amin. 2009. Multifrequency-based range estimation of RFID tags. In *2009 IEEE International Conference on RFID*. IEEE, 147–154.
- [29] Yunfei Ma, Nicholas Selby, and Fadel Adib. 2017. Minding the billions: Ultra-wideband localization for deployed rfid tags. In *Proceedings of the 23rd Annual International Conference on Mobile Computing and Networking*. ACM, 248–260.
- [30] Guoqiang Mao, Barış Fidan, and Brian DO Anderson. 2007. Wireless sensor network localization techniques. *Computer networks* 51, 10 (2007), 2529–2553.
- [31] Andreas Marceletti, Maurizio Rea, Domenico Giustiniano, Vincent Lenders, and Aymen Fakhreddine. 2014. Filtering noisy 802.11 time-of-flight ranging measurements. In *Proceedings of the 10th ACM International on Conference on emerging Networking Experiments and Technologies*. ACM, 13–20.
- [32] Alex T Mariakakis, Souvik Sen, Jeongkeun Lee, and Kyu-Han Kim. 2014. Sail: Single access point-based indoor localization. In *Proceedings of the 12th annual international conference on Mobile systems, applications, and services*. ACM, 315–328.
- [33] Robert Miesen, Fabian Kirsch, and Martin Vossiek. 2011. Holographic localization of passive UHF RFID transponders. In *RFID (RFID), 2011 IEEE International Conference on*. IEEE, 32–37.
- [34] John C Mosher and Richard M Leahy. 1999. Source localization using recursively applied and projected (RAP) MUSIC. *IEEE Transactions on signal processing* 47, 2 (1999), 332–340.
- [35] Lionel M Ni, Yunhao Liu, Yiu Cho Lau, and Abhishek P Patil. 2003. LANDMARC: indoor location sensing using active RFID. In *Proceedings of the First IEEE International Conference on Pervasive Computing and Communications, 2003.(PerCom 2003)*. IEEE, 407–415.
- [36] Dragoş Niculescu and Badri Nath. 2004. VOR base stations for indoor 802.11 positioning. In *Proceedings of the 10th annual international conference on Mobile computing and networking*. ACM, 58–69.
- [37] Ralph Schmidt. 1986. Multiple emitter location and signal parameter estimation. *IEEE transactions on antennas and propagation* 34, 3 (1986), 276–280.
- [38] Souvik Sen, Jeongkeun Lee, Kyu-Han Kim, and Paul Congdon. 2013. Avoiding multipath to revive inbuilding WiFi localization. In *Proceeding of the 11th annual international conference on Mobile systems, applications, and services*. ACM, 249–262.
- [39] Tie-Jun Shan, Mati Wax, and Thomas Kailath. 1985. On spatial smoothing for direction-of-arrival estimation of coherent signals. *IEEE Transactions on Acoustics, Speech, and Signal Processing* 33, 4 (1985), 806–811.
- [40] Elahe Soltanaghaei, Avinash Kalyanaraman, and Kamin Whitehouse. 2017. Peripheral wifi vision: Exploiting multipath reflections for more sensitive human sensing. In *Proceedings of the 4th International on Workshop on Physical Analytics*. 13–18.
- [41] Elahe Soltanaghaei, Avinash Kalyanaraman, and Kamin Whitehouse. 2017. Poster: Improving multipath resolution with MIMO smoothing. In *Proceedings of the 23rd Annual International Conference on Mobile Computing and Networking*. 585–587.
- [42] Elahe Soltanaghaei, Avinash Kalyanaraman, and Kamin Whitehouse. 2018. Multipath triangulation: Decimeter-level wifi localization and orientation with a single unaided receiver. In *Proceedings of the 16th Annual International Conference on Mobile Systems, Applications, and Services*. ACM, 376–388.
- [43] Elahe Soltanaghaei, Rahul Anand Sharma, Zehao Wang, Adarsh Chittilappilly, Anh Luong, Eric Giler, Katie Hall, Steve Elias, and Anthony Rowe. 2020. Robust and Practical WiFi Human Sensing Using On-device Learning with a Domain Adaptive Model. In *Proceedings of the 7th ACM International Conference on Systems for Energy-Efficient Buildings, Cities, and Transportation*. 150–159.
- [44] Xinyu Tong, Fengyuan Zhu, Yang Wan, Xiaohua Tian, and Xinbing Wang. 2019. Batch Localization Based on OFDMA Backscatter. *Proceedings of the ACM on Interactive, Mobile, Wearable and Ubiquitous Technologies* 3, 1 (2019), 25.
- [45] MC Vanderveen, BC Ng, CB Papadias, and A Paulraj. 1996. Joint angle and delay estimation (JADE) for signals in multipath environments. In *Conference Record of the Thirtieth Asilomar Conference on Signals, Systems and Computers*. IEEE, 1250–1254.
- [46] Hubregt J Visser, Adrianus CF Reniers, and Jeroen AC Theeuwes. 2008. Ambient RF energy scavenging: GSM and WLAN power density measurements. In *2008 38th European Microwave Conference*. IEEE, 721–724.
- [47] Jue Wang, Fadel Adib, Ross Knepper, Dina Katabi, and Daniela Rus. 2013. RF-compass: Robot object manipulation using RFIDs. In *Proceedings of the 19th annual international conference on Mobile computing & networking*. ACM, 3–14.
- [48] Jue Wang and Dina Katabi. 2013. Dude, where’s my card?: RFID positioning that works with multipath and non-line of sight. In *ACM SIGCOMM Computer Communication Review*, Vol. 43. ACM, 51–62.
- [49] John Wang and Edwin Olson. 2016. AprilTag 2: Efficient and robust fiducial detection. In *2016 IEEE/RSJ International Conference on Intelligent Robots and Systems (IROS)*. IEEE, 4193–4198.
- [50] Kaishun Wu, Jiang Xiao, Youwen Yi, Min Gao, and Lionel M Ni. 2012. Fila: Fine-grained indoor localization. In *2012 Proceedings IEEE INFOCOM*. IEEE, 2210–2218.

- [51] Yaxiong Xie, Jie Xiong, Mo Li, and Kyle Jamieson. 2016. xD-track: leveraging multi-dimensional information for passive wi-fi tracking. In *Proceedings of the 3rd Workshop on Hot Topics in Wireless*. 39–43.
- [52] Jie Xiong and Kyle Jamieson. 2013. Arraytrack: A fine-grained indoor location system. In *Presented as part of the 10th {USENIX} Symposium on Networked Systems Design and Implementation ({NSDI} 13)*. 71–84.
- [53] Jie Xiong, Karthikeyan Sundaresan, and Kyle Jamieson. 2015. Tonetrack: Leveraging frequency-agile radios for time-based indoor wireless localization. In *Proceedings of the 21st Annual International Conference on Mobile Computing and Networking*. 537–549.
- [54] Lei Yang, Yekui Chen, Xiang-Yang Li, Chaowei Xiao, Mo Li, and Yunhao Liu. 2014. Tagoram: Real-time tracking of mobile RFID tags to high precision using COTS devices. In *Proceedings of the 20th annual international conference on Mobile computing and networking*. ACM, 237–248.
- [55] Moustafa Youssef, Adel Youssef, Chuck Rieger, Udaya Shankar, and Ashok Agrawala. 2006. Pinpoint: An asynchronous time-based location determination system. In *Proceedings of the 4th international conference on Mobile systems, applications and services*. ACM, 165–176.
- [56] Pengyu Zhang, Dinesh Bharadia, Kiran Joshi, and Sachin Katti. 2016. Hitchhike: Practical backscatter using commodity wifi. In *Proceedings of the 14th ACM Conference on Embedded Network Sensor Systems CD-ROM*. ACM, 259–271.
- [57] Pengyu Zhang, Colleen Josephson, Dinesh Bharadia, and Sachin Katti. 2017. Freerider: Backscatter communication using commodity radios. In *Proceedings of the 13th International Conference on emerging Networking EXperiments and Technologies*. ACM, 389–401.
- [58] Pengyu Zhang, Mohammad Rostami, Pan Hu, and Deepak Ganesan. 2016. Enabling practical backscatter communication for on-body sensors. In *Proceedings of the 2016 ACM SIGCOMM Conference*. ACM, 370–383.
- [59] Jia Zhao, Wei Gong, and Jiangchuan Liu. 2018. Spatial Stream Backscatter Using Commodity WiFi. In *Proceedings of the 16th Annual International Conference on Mobile Systems, Applications, and Services*. ACM, 191–203.
- [60] Junyi Zhou and Jing Shi. 2009. RFID localization algorithms and applications—a review. *Journal of intelligent manufacturing* 20, 6 (2009), 695.
- [61] Junru Zhou, Hongjian Zhang, and Lingfei Mo. 2011. Two-dimension localization of passive RFID tags using AOA estimation. In *2011 IEEE International Instrumentation and Measurement Technology Conference*. IEEE, 1–5.